

**OPTIMAL LOAD SHEDDING IN PRESENCE OF  
RENEWABLE SOURCES: A WIND STUDY CASE**

BY

**SHAKIR DAWALBAIT AHMED MOHAMMED**

A Thesis Presented to the  
DEANSHIP OF GRADUATE STUDIES

**KING FAHD UNIVERSITY OF PETROLEUM & MINERALS**

DHAHRAN, SAUDI ARABIA

In Partial Fulfillment of the  
Requirements for the Degree of

**MASTER OF SCIENCE**

In

**ELECTRICAL ENGINEERING**

**MAY, 2016**

KING FAHD UNIVERSITY OF PETROLEUM & MINERALS

DHAHRAN- 31261, SAUDI ARABIA

**DEANSHIP OF GRADUATE STUDIES**

This thesis, written by SHAKIR DAWALBAIT AHMED under the direction his thesis advisor and approved by his thesis committee, has been presented and accepted by the Dean of Graduate Studies, in partial fulfillment of the requirements for the degree of **MASTER OF SCIENCE IN ELECTRICAL ENGINEERING.**

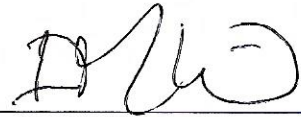


Dr. ALI AHMED AL-SHAIKHI  
Department Chairman



Dr. Salam A. Zummo  
Dean of Graduate Studies

16/8/16  
Date



Dr. IBRAHIM M. EL-AMIN  
(Advisor)



Dr. MOHAMMED A. ABIDO  
(Member)



Dr. M. M. ALMUHAINI  
(Member)

© SHAKIR DAWALBAIT AHMED

2016

*Dedicated to my Family*

## **ACKNOWLEDGEMENT**

Firstly, I would like to express my sincere appreciation to my advisor Prof. Ibrahim Mohamed El-Amin for his support in my MS study and the thesis work, for his patience, incentive, and immense knowledge. His guidance helped me in all the time of research and writing of this thesis.

Besides my advisor, I would like to thank the rest of my thesis committee: Prof. Mohammed Abido, and Dr. Mohammad Al-Muhaini, for being part of my thesis committee and their valuable comments on my subject work

Also, I thank my friends in the following institutions, Electrical engineering, and System engineering specially Mr. Aman Abdullah for his support in writing the codes.

Last but not the least, I would like to thank my family: my parents and to my brothers and sister for supporting me spiritually throughout writing this thesis and my life in general.

# TABLE OF CONTENTS

ACKNOWLEDGMENTS.....	V
TABLE OF CONTENTS.....	VI
LIST OF TABLES.....	IX
LIST OF FIGURES.....	X
LIST OF ABBREVIATIONS.....	XII
ABSTRACT.....	XIII
ملخص الرسالة.....	XIV
CHAPTER 1 INTRODUCTION.....	1
1.1 Research Motivation.....	4
1.2 Objective of the Research .....	5
1.3 Overview of the thesis .....	5
CHAPTER 2 LITERATURE REVIEW .....	6
2.1 Introduction.....	6
2.2 Under Frequency Load Shedding.....	6
2.3 Under Voltage Load Shedding .....	14
CHAPTER 3 MODELING AND RESEARCH METHODOLOGY .....	20
3.1 Introduction.....	20
3.2 Problem Formulation .....	20
3.2.1 Objective function .....	21
3.2.2 Generation constraints.....	22

3.2.3	Load constraints .....	22
3.2.4	Load flows equations.....	23
3.3	System Model .....	25
3.3.1	Generator model .....	25
3.3.2	Governor model .....	27
3.3.3	Exciter model .....	29
3.3.4	Wind turbine model .....	30
3.3.5	Load modelling.....	32
3.4	Optimization Methods .....	34
3.4.1	Basic fundamentals of PSO algorithm.....	36
3.5	The procedure for load shedding .....	40
<b>CHAPTER 4 RESULTS AND DISCUSSION .....</b>		<b>43</b>
4.1	Study system 1: WECC 9 bus system .....	43
4.1.1	Conventional load shedding .....	45
4.1.2	Optimal load shedding with reserve .....	47
4.1.3	Comparison with published work on optimal load shedding .....	51
4.1.4	Loss of transmission line 4-5 in WECC 9 bus system.....	52
4.2	Study system of WECC 9 bus in the presence of wind turbine. ....	55
4.2.1	Conventional load shedding. ....	57
4.2.2	Optimal load shedding with reserve .....	59
4.3	Study system 2: New England 39 bus system .....	62
4.3.1	Conventional load shedding .....	64
4.3.2	Optimal load shedding .....	65
4.3.3	Case 5 loss transmission lines 5-8 and 7-8 .....	69
4.4	Study system of New England 39 bus system in presence of wind turbine .....	72

4.4.1	Conventional load shedding results .....	73
4.4.2	Optimal load shedding results .....	74
<b>CHAPTER 5 CONCLUSION.....</b>		<b>77</b>
5.1	Conclusion .....	77
5.2	Future works.....	78
<b>REFERENCES.....</b>		<b>79</b>
<b>APPENDICES .....</b>		<b>82</b>
<b>VITAE.....</b>		<b>95</b>



## LIST OF TABLES

Table 4.1. Conventional load shedding setting.....	45
Table 4.2 Bus output data for a healthy IEEE 9 bus system.....	47
Table 4.3 Bus output data for IEEE 9 bus system after loss generator 2 and shedding scheme work.....	47
Table 4.4. Optimal Under frequency load shedding -- Frequency Threshold—59.6. ....	48
Table 4.5 Comparison between two optimal load shedding schemes when generator 2 loss 100 MW .....	52
Table 4.6 Bus output data for WECC 9 bus system after loss generator 2 and shedding scheme work in the presence of wind. ....	59
Table 4.7 Percentage load shedding after loss generator 9 in IEEE 39 bus system .....	66
Table 4.8. Load shed results .....	70
Table 4.9. Load shedding results .....	75

## LIST OF FIGURES

Figure 2.1 Frequency decay due to generation deficiency .....	8
Figure 2.2. Illustration for integrating ROCHOF .....	9
Figure 2.3. Example P-V curve.....	15
Figure 2.4. Difficulties in Coordinating UVLS Pickup Setting, a) difficulty to keep security (unwanted UVLS responding to normal condition) b) difficulty to keep dependability (Load shedding after system passing nose). .....	16
Figure 3.1. GENROU without Saturation [28] .....	26
Figure 3.2. Steam Turbine-Governor Model TGOV1 .....	28
Figure 3.3. Block diagram for IEEE1 exciter.....	29
Figure 3.4. Wind turbine model DFAG [28]. .....	31
Figure 3.5. Load Characteristics CLOD [28].....	33
Figure 3.6. The algorithm for PSO .....	39
Figure 3.7. Optimal load shedding diagram.....	40
Figure 4.1. WSCC 9 bus test system.....	43
Figure 4.2 Frequency response without load shedding.....	44
Figure 4.3 Frequency response due to conventional load shedding .....	45
Figure 4.4 Voltages at load bus after conventional load shedding .....	46
Figure 4.5 Frequency response at bus 7 for load shedding with reserve .....	48
Figure 4.6 Voltages at load buses after load shedding.....	49
Figure 4.7. Comparison between frequencies at each case.....	50
Figure 4.8. Voltage at load bus 8 in all cases.....	50
Figure 4.9. Total load shed in each load shedding scheme.....	51
Figure 4.10. Load voltage after loss line 4-5 .....	53
Figure 4.11. Frequency response after loss of transmission line .....	53
Figure 4.12. Load voltages after load shedding .....	54
Figure 4.13. Frequency response at bus 7 after load shedding .....	55
Figure 4.14. WSCC 9 bus system with wind turbine.....	56
Figure 4.15. Frequency response in the presence of wind .....	57
Figure 4.16. Frequency response in conventional load shedding .....	58
Figure 4.17. Load voltages after load shedding.....	59
Figure 4.18. Bus 7 frequency response after load shedding .....	60
Figure 4.19. Load voltages after load shedding.....	61
Figure 4.20. New England 39 bus system.....	62
Figure 4.21 Frequency at bus 2 following major disturbance without load shedding .....	63
Figure 4.22. Frequency response after conventional load shedding .....	64
Figure 4.23. Load voltage after conventional load shedding.....	65
Figure 4.24 Frequency response after optimal load shedding. ....	67
Figure 4.25. Load voltages after load shedding.....	68
Figure 4.26. Load shed comparison.....	68

Figure 4.27. Load voltage due to lines loss .....	69
Figure 4.28. Frequency response due to lines loss.....	70
Figure 4.29. Load voltage after load shedding .....	71
Figure 4.30. Frequency response after load shedding.....	71
Figure 4.31. Frequency response during major disturbance in presence of wind.....	72
Figure 4.32. Frequency response after load shedding.....	73
Figure 4.33. Load voltage after load shedding .....	74
Figure 4.34. Frequency response after load shedding.....	76
Figure 4.35. Load voltage after load shedding .....	76
Figure C.1 Loss 163 MW From generator 2.....	92
Figure C.2 Loss 100 MW cost function.....	92
Figure C.3 Loss 163 MW in presence of wind .....	93
Figure C.4 Loss transmission line 4-5 .....	93
Figure C.5 Loss generator 9 in 39 bus system .....	94
Figure C.6 Loss generator 9 in 39 bus system in presence of wind.....	94
Figure C.7 Loss transmission lines 5-8 and 7-8.....	94

## **LIST OF ABBREVIATIONS**

<b>UFLS</b>	:	Under Frequency Load Shedding
<b>UVLS</b>	:	Under Voltage Load Shedding
<b>ROCOF</b>	:	Rate of Change of Frequency
<b>WSCC</b>	:	Western System Coordinating Council
<b>DGs</b>	:	Distributed Generators
<b>PSO</b>	:	Particle Swarm optimization

## **ABSTRACT**

Full Name : SHAKIR DAWALBAIT AHMED MOHAMMED

Thesis Title : Optimal Load Shedding in Presence of Renewable Sources: A Wind Study Case

Major Field : Electrical Engineering

Date of Degree : May 2016

Electric utilities face increasing energy demand while the generation capacity is constrained and limited. System operators in many instances are obliged to shed off loads to maintain the balance between generation and load. Load shedding (LS) is defined as a technique of reducing demand (load) on the generation system by temporarily switching off some nonessential loads. The current methods used in load shedding are under-voltage and under-frequency schemes. These may unnecessarily switch some loads to maintain the frequency or voltage.

The proposed method combine both frequency and voltage in an objective function. The objective function is solved using Particle Swarm Optimization (PSO). The formulation is tested using WECC 9 bus and IEEE New England 39 bus systems. Emergence of renewable energy sources especially wind power is addressed in this research. Contingency studies such loss of major generation, outage of critical line etc. were conducted. The study cases showed the successful implementation of the load shedding scheme and its ability to maintain both frequency and voltage within operation limits. The results indicate superior performance over the conventional schemes. Where in these techniques, if the frequency is lower than the given thresholds (divided into steps), the load shedding will then be implemented.

## ملخص الرسالة

الاسم الكامل: شاكر ضوالبيت احمد محمد

عنوان الرسالة: تقليص الاحمال الامثل في وجود الموارد المتجددة : الرياح كدراسة حالة

التخصص: الهندسة الكهربائية

تاريخ الدرجة العلمية: مايو 2016

تواجه شركات الكهرباء طلب متزايد علي الطاقة, في حين أن انتاج الطاقة محدود بقيود إقتصادية وغيرها. يقوم مشغلي المحطات في بعض الاوقات بقطع الامداد من بعض المستهلكين للحفاظ علي التوازن بين الطلب والانتاج. عملية تقليص الحمل الكهربائي هي طريقة متبعة لتقليل الطلب علي الكهرباء بفصل الطاقة من الاحمال الغير ضرورية. الطرق المستخدمة حاليا في عملية تقليص الاحمال الكهربائية هي : تقليص الاحمال عند هبوط الجهد, او تقليص الاحمال عند هبوط التردد. في الطرق المذكورة اعلاة قد يتم فصل أحمال من دون الحاجة الي ذلك لإرجاع التردد او الجهد الي مستوي التشغيل.

الطريقة المقترحة تربط بين الجهد والتردد في معادلة واحدة . خوارزمية استمثال عناصر السرب تم استخدامها في حل هذه المسألة. هذه الصيغة تم اختبارها علي منظومتي قوي كهربائية, منظومة اختبار مكونة من تسع قضبان توصيل و المنظومة الاخرى مكونة من 39 قضبان توصيل. بروز مصادر الطاقة المتجددة في منظومة القوي الكهربائية خصوصا طاقة الرياح تم إعتبارها في هذا البحث. تم تطبيق خطط الطوارئ مثل, فقد محطة توليد حيوية أو خط نقل قوي رئيسي. اظهرت النتائج نجاح الطريقة المقترحة لتقليص الحمل ومقدرتها علي الحفاظ علي الجهد والتردد في الحدود التشغيلية المسموح بها. وتشير النتائج إلى الأداء المتفوق للطريقة المقترحة على الطرق التقليدية. والتي يتم فيها تقليص الاحمال علي عدة مراحل بناء علي قيم للجهد او التردد مضبوطة مسبقا.

# CHAPTER 1

## INTRODUCTION

These days, power utilities transfer electricity increasingly to vast areas. This large growth in the electrical industry also has an effect on the system performance. A small disturbance in any location can affect the entire system. Besides that, the economic condition and market competition have forced electric utilities to operate power system close to the limits with a minimum reserve. Thus, a minor disturbance can cause voltage and frequency problems throughout the power system. This mode of operation caused and resulted in many blackouts and outages in a number of networks and countries. In addition, the increased penetration of renewable energy presents system operators with further challenges.

To investigate system outages, there is need to define the operation states of the power system. The power system has different operation states and can be classified into normal and abnormal (disturbance) operation states. In the normal operating state, all the constraints are met such as power flows in the lines, voltages at buses and the frequency. In this state a minor disturbance in the system can be overcome. The basic control in the power system can handle this disturbance.

Under large disturbance events (abnormal state), the system operates at emergency state. The system still keeps its integrity at that point but within acceptable limits for some system variables, namely the voltages and frequency and even power flow. If the control systems

are unable to mitigate this situation and it persists, the condition may be aggravated and a widespread blackout can occur [1].

The mismatch in the active power between generation and demand has a direct impact on the network frequency. The imbalance in the active power of the system at any point will be reflected in a frequency increase or decrease. Each generating unit is equipped with a speed governor to provide primary speed control, as well as additional features in the control center for distributing generation [1].

It is understood that the main goal of generation controls is to achieve a balance between the generation and system load. Generation and transmission controls working side by side to keep voltage and frequency of power system within acceptable operating levels. Load-frequency control attempts to keep a constant frequency and thus speed stability in synchronous and induction motors. Substantial frequency drop in the network may result in high magnetization current in transformers and induction motors according to Faraday's law [2]. The use frequency for timing purposes and electric clocks requires careful maintenance for time synchronization.

Severe network disturbances can bring about blackouts and isolation of regions, creating the formation of electrical islands. In the event that such an islanded zone is under-generated, it will encounter a frequency drop. Unless adequate generation with the capacity to quickly build output is accessible, the decrease in frequency will be to a great extent dictated by frequency sensitive characteristics of loads. In severe situations, the under-frequency protective relays could early trip turbine generating units due to the decline in the frequency, causing further decrease [3].



To avoid partial or complete blackouts, system operators tend to disconnect loads in a controlled manner. This is done to minimize the damage and the consequence of a blackout. System operators try to shed off some load in response to voltage and frequency decline. An intentional power outage is defined as rotational load shedding (LS) or feeder rotation is a deliberately designed shutdown where power conveyance is ceased for a non-covering time. Planned power outages are a final resort measure utilized by a power system company to evade a serious power outage of the system. This is a kind of demand response for a circumstance where the demand for power surpasses the supply ability of the system. Power outages may be restricted to a particular portion of the power system or may be broader and influence whole nations and continents. Intentional power outages, for the most part, occur for two reasons: inadequate generation capacity or lack of transmission facilities to transfer sufficient power to the zone where it is required [1].

However, many questions arise such as where, how much and when to shed off loads. Traditional load shedding is based on using the under frequency and under voltage schemes. The schemes are based on load priority and other factors.

In a power system, frequency and voltage are used as a measure of a balance of MW and MAVr respectively between generation and load. From above relation, there are two schemes of load shedding: under frequency load shedding (UFLS) and under voltage load shedding (UVLS).

In the case of losing generation or part of it for any reason, it is essential to reduce some of the load to create a balance between generations and loads. During this situation, the frequency will decline to lower values than operating reference (60 or 50) Hz. This is called

under frequency problem. Under frequency problems mandate a protection solution to prevent frequency decline by shedding off some load in an orderly manner. This action will elevate the situation and prevent more outages [4].

Similarly, there is a load-shedding scheme to prevent voltage collapse in the power system, known as under-voltage load shedding. The idea of UVLS stated as follows: when a disturbance occurs and the voltage drops to a threshold value with specified delay time, some loads will be dropped. The result of the above process is recovering voltage to operation limits, thereby avoiding deterioration the voltage throughout the system[5], [6].

## **1.1 Research Motivation**

Many publications and works have addressed the problem of load shedding. The research on the problem of optimal load shedding usually designed depending on the frequency alone or voltage alone but the combination of the two scheme is not widely addressed. In this research, the problem of load shedding is addressed as a joint optimal issue. The objective is to find the appropriate amount of load to be shed, location and the instant at which the shedding takes place.

Few publications addressed load shedding including renewable resources. In this research, the load shedding is applied to the system including wind turbine. The purpose is to study the effect of the wind turbine on load shedding scheme.

## **1.2 Objective of the Research**

The general objective of this study is to develop optimal load shedding that can be used in case of under frequency or under voltage events.

The expected outcomes of this research are as follows:

- Develop an optimum load shedding strategy.
- Consider a combined frequency-voltage load shedding techniques.
- Incorporate renewable resources (i.e. wind) into the available generation.
- Apply the developed model on typical power systems.

The optimal problem is solved using Particle Swarm Optimization (PSO) method. MATLAB software is used for the implementation. Powerworld Simulator has been used for system dynamic analysis before and after load shedding.

## **1.3 Overview of the thesis**

The contents of this thesis are distributed into five chapters. Chapter one is devoted to a problem introduction and research motivation. Chapter two reviews the literature related to under frequency and under-voltage load shedding. Chapter three contains the problem formulation and solution methodology. Chapter four deals with results and the study cases to illustrate the validity of the developed model. Finally, chapter five contains the conclusions and suggestions for future work

## **CHAPTER 2**

### **LITERATURE REVIEW**

#### **2.1 Introduction**

Secure power system operation is the cornerstone of the electricity industry. Balanced generation and load result in providing consumers with constant voltage and frequency. Many research works address and suggest means to maintain system stability following major disturbances or outages. Decline and reduction of voltage or frequency are an indication of system instability. Load shedding scheme is one of the measures adopted by the system operator to avoid major outages and blackouts.

The following sections present a review of the research work performed in the area of load shedding.

#### **2.2 Under Frequency Load Shedding**

Under-frequency-load-shedding is a known technique to prevent system frequency dropping to an unacceptable level and is widely used by electrical utilities. The main purpose of Under Frequency Load Shedding is to achieve a balance between generation

and load following a disturbance in a system and to avoid a substantial decline in system frequency. The decline in frequency can result in the establishment of islanded networks.

Electrical islands can be created due to major instabilities in networks that make cascading outages and isolated areas. In case the generation in these areas is insufficient to pick up the areas load, this will lead to frequency decline. This decline will be larger if there is no reserve available at the time of the event with the capability to quickly increase the output. If the frequency reaches limits of under frequency protective relay setting of a generating unit, this may lead to tripping the unit and deteriorate the situation. Load Shedding or Under Frequency Load Shedding (UFLS) can play a major role in avoiding the operation of islanded areas at a lower frequency. Load shedding intends to decrease the connected load such that the generation can supply securely[1].

If the spinning reserve for the separated areas is insignificant, the amount of frequency deviation and the rate of decline that may be encountered in separated areas are determined mainly by three elements: generation deficiency ( $\Delta L$ ), Load damping constant ( $D$ ), and lastly the inertia constant ( $M$ ) which is the total inertia of the area generations [1]. Figure 2.1 shows the effect of generation deficiency on the frequency decline for a constant system inertia and load damping.

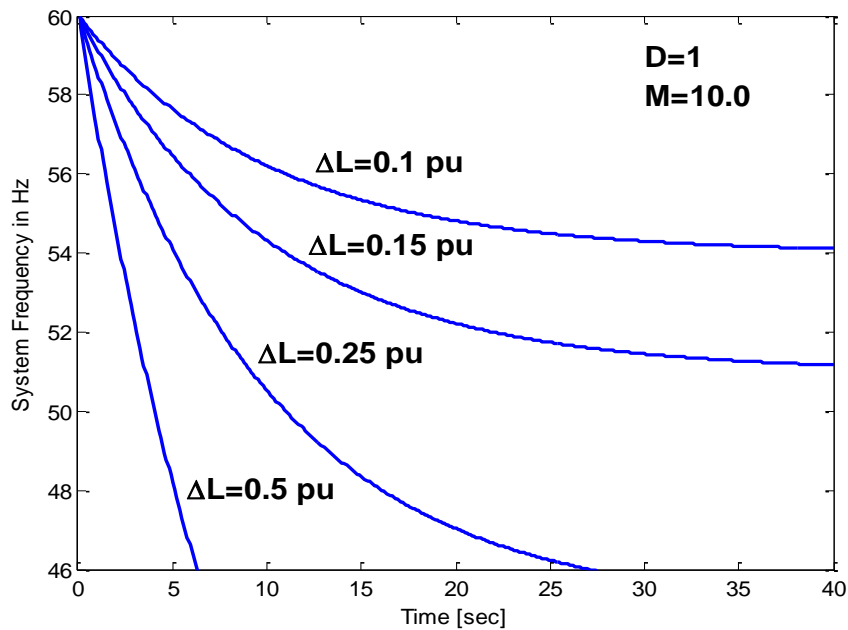


Figure 2.1 Frequency decay due to generation deficiency

Figure 2.1 can be the useful starting point for developing load shedding scheme [1].

The typical conventional under-frequency load shedding steps [1]:

- If the frequency drops to 59.2 Hz shed 10% of the load
- If the decline reaches 58.8 Hz shed extra 15% of the load
- And if it drops to 58 Hz shed 20% of the load

The rate of change of the frequency (ROCOF) is used to determine the extent of frequency drop in a degenerated area. This measure cannot provide the actual amount of load to be shed because ROCOF has oscillatory nature.

Zhang & Zhong [7], proposed to use the rate of change of frequency (ROCOF) as a supplementary measure for under frequency scheme design. The authors integrate the dynamic frequency between consecutive times. They avoid the oscillatory problem associate with direct ROCOF. The authors use five step under frequency load shedding to illustrate their work. But if the oscillation is large more steps may be needed. Figure 2.2 describes the idea of integrating ROCOF. S1, S2, S3, and S4 represents the integrating values, the interval for this case 2 seconds.

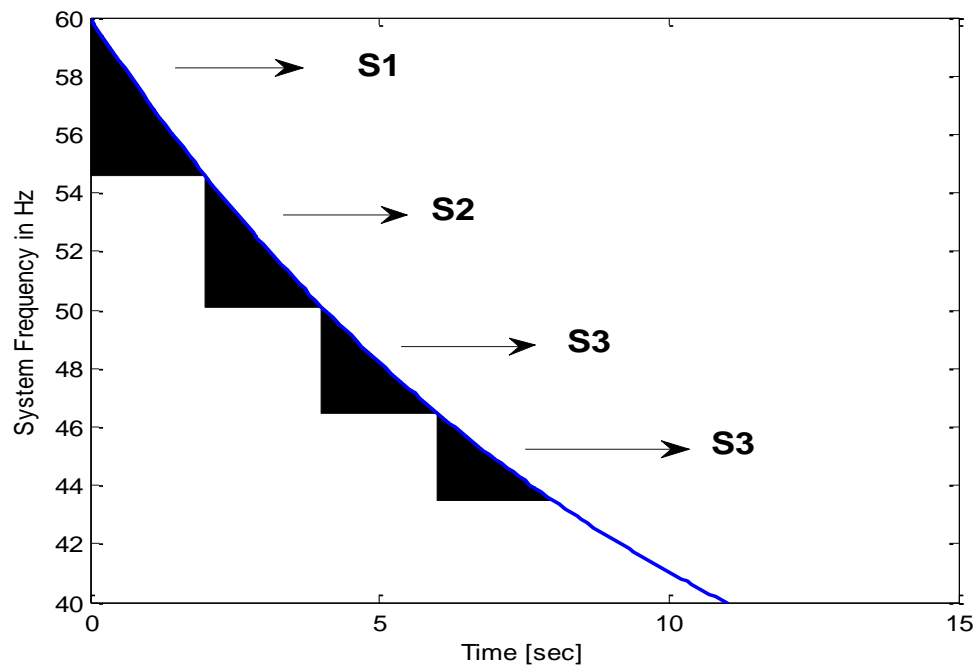


**Figure 2.2. Illustration for integrating ROCOF**

To improve the under frequency load shedding new approaches have been developed by researchers namely adaptive and intelligent scheme. Adaptive load shedding using information of rate of change of frequency and local frequency is reported [8]. An Intelligent automated load shedding is presented [9].

Joshi [10] developed load shedding taking into consideration the information of voltage and frequency in determining the amount of load to be shed and load distribution between load buses. The idea of the scheme is as the same the under frequency load shedding using the frequency and rate of change of frequency to determine disturbance quantity. The amount of load to be shed at each bus is decided by the degree of voltage deviation. The idea resemblances the adaptive scheme presented in [10].

Tang et al. [11] proposed load shedding scheme based on combined voltage and frequency information to overcome shortcomings of adaptive load shedding. The synchrophasor is deployed in the measurement process through their work. The authors consider reactive power in load shedding accompanied with active power. This ensures voltage stability after load shedding successfully. Voltage dependency load model is applied in this scheme to address stability problem in a precise way. Beside synchrophasor measurements, also, load flow tracing algorithm is used for buses selectivity for load shedding. An RDTS is used to simulate the test system and MATLAB for offline calculation.

The under frequency load shedding can be divided into static and dynamic schemes. The static, as the name implies, sheds a constant amount of load each time. In the dynamic scheme, the value to be shed depends on the degree of imbalance and rate of change of frequency. Zin et al. [12] carried out a study for both static and dynamic load shedding and compared the finding of the design. The outcomes are:

- 1) The static scheme takes more steps and longer time for the frequency to settle down.
- 2) In the dynamic scheme, the frequency stabilizes quicker, and the step of shedding depends on the imbalance power. The scheme shed even less load.



Mokhlis et al. [13] proposed a new approach for under frequency load shedding to resolve the problem of under frequency and stability in the separated areas for the distribution system. The authors implement the adaptive and intelligent technique in the proposed work. The schemes use two approaches: 1) response-based and 2) event-based to decide the amount of load to be curtail. The quantity of load to be shed in the event-based is estimated by using power difference. The response-based load sheds uses three components: swing equation, online frequency, and the rate of change of the frequency. To test the efficiency and strength of the model, the authors applied two scenarios. The first one is at beginning of the formation of islands in the distribution system. The second one for different events after the islands was formed such as loading condition or faults.

The model did the role of automated load shedding and differentiated between the two types (i.e. events based and response-based). The schemes show a good response to the events and can prevent losing the island [13].

Abdelwahid et al. [14], with the help of actual hardware implementation, developed an adaptive centralized UFLS in real-time. The hardware is Phasor Measurements Units PMUs, a synchro phasor vector processor (SVP), and a real-time digital simulator (RTDS). The objective is to prevent frequency decline and to validate the model in real time. The scheme used the same relationship mentioned in [13] to determine the amount of load to be curtailed and taking into account the voltage status at buses to distribute the load shed between buses.

Xia et al.[15], proposed adaptive under frequency load shedding based on the integration of real time frequency information and traditional state Estimator (SE). The scheme falls under the Wide Area Monitoring, protection and Control (WAMPAC) area for a smarter transmission system. The frequency dynamic is traced during contingency using fast sampled frequency measurements. The mathematical problem solution is approximated to cope with real time. The scheme is tested in two typical power networks to demonstrate its validity [15].

Wu [16], proposed a multi-agent-based distributed load shedding scheme for micro-grids. The authors use average-consensus to gather system information (frequency/ voltage). The weights of load shedding are evaluated locally on the cost and capacity of the load. The transient analysis is carried out on (PSCAD/EMTDC) to validate the proposed scheme[16]

Palaniswamy & Sharma [17] proposed optimal load shedding based on three parameters, generator control effects, frequency and voltage characteristics of the loads. The scheme depends on the load flow principles. Second order technique had been used to solve the optimization objective function. The load model includes frequency and voltage characteristics.

Adel A. Abou-El-Ela et al. [18] introduced an optimal proposed procedure (OPP) to regain stable situation if there is a power imbalance between generation and load. The scheme is divided into three stages. The first stage devoted to calculating the balance between generation and demand and it contains three objective functions. The first one deals with load priority in the load shedding process. The second one minimizes the load to be curtailed, and the last one minimizes the system transmission loss. Stage two is designed

for load restoration and has two objective functions for load priority and maximizes the amount of load to be reconnected to the network. The last stage is carried out after the system reaches secure operation level which has one objective to re-dispatch the available generation. The constraints applied to the above-mentioned objective function are the system flows and system security limits. To solve the problems multi-objective genetic algorithm was applied [18].

Çimen [19], proposed intelligent optimal load shedding strategy. In this scheme, the load is sorted by importance priority. The fuzzy logic technique is used to solve the mathematical problem. The scheme is applied on university premises [19].

Mageshvaran & Jayabarathi [20], proposed a new approach of steady state optimal load shedding based on improved harmony search algorithm (IHSA). The scheme uses the same techniques used in [16], [19] to decide the load to be curtailed. The scheme implements both active and reactive load in the load shedding estimation.

Liu et al. [21] developed optimal under frequency load shedding approach to study the effect of distributed generators (DGs) on the load shedding. The proposed work assumed that the system under study is fully equipped with advanced distribution management system (DMS) to give real time information regarding spinning reserve and other power system components. The design structure is divided into two rounds named basic round and special round. The basic round uses the adaptive under frequency technique to relieve the frequency deviation. The special round is implemented to remove any fluctuation of settling for the frequency at points other than operation frequency. In the special round, the optimization program is performed and the distributed generators (DGs) contribution is

considered. The objective function formulated in the special round, intends to minimize voltage and frequency deviations in addition to the amount of load that will be shed in this round.

Most of the research in this group follows the rate of change of frequency (ROCOF) technique to decide the amount of load to be shed. This is unreliable measure because the frequency decay is oscillatory in nature. This may lead to shed more or less load. Most of the literature ignores the voltage effect due to load shedding.

### **2.3 Under Voltage Load Shedding**

Under-voltage-load-shedding is difficult to design compared to under frequency load shedding. This involves a full coordination between two entities, system protection, and operation. The UVLS deployed by the utility can be divided into two types: centralized and decentralized (distributed).

Both types are in use by the electrical utilities. The idea of decentralized UVLS is that the load is equipped with the relays. If an under voltage is encountered at this position the relay will take action by shedding this load. In the case of centralized UVLS, the under voltage relay will be at main load buses. The trip signal will be sent to individual loads at the various locations when the under voltage is detected[5].

Mozina [5] argued the considerations that should be taken to design and develop a secure under-voltage load shedding system. The first stage, for good voltage collapse scenarios, the P-V curves needs to be defined.

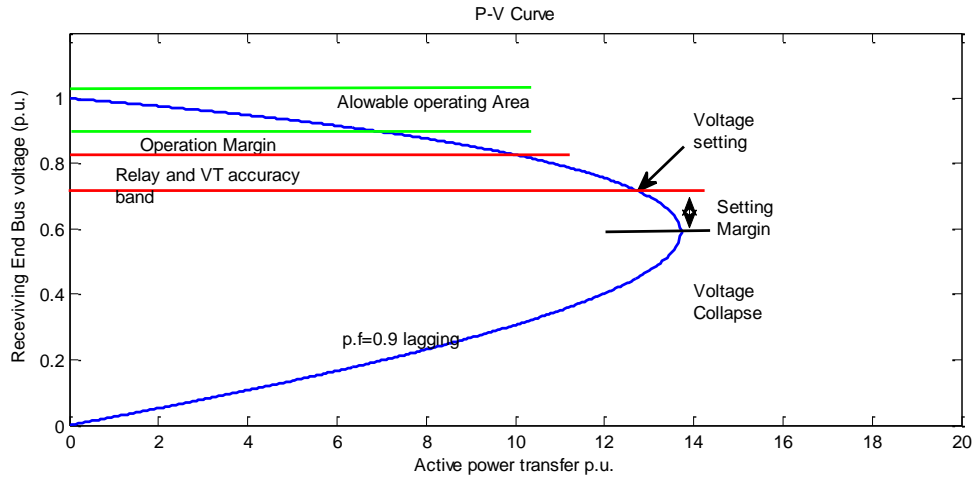


**Figure 2.3. Example P-V curve**

Figure 2.3 shows an example P-V curve for a credible contingency. The knee of the curve at which the voltage will collapse is identified as collapse. A setting margin or safety factor is desired and then the accuracy band of the relay and VT is shown. The setting (V setting) must be set above these margins. As with all relay settings, dependability and security need to be balanced. If too small a margin is chosen, there is a risk of the scheme operating during allowable emergency conditions that do not yet require load shedding. If too small a margin is chosen, then load shedding could occur after the system passes below the nose curve voltage collapse point (V collapse) shown in Figure 2.3 [5].

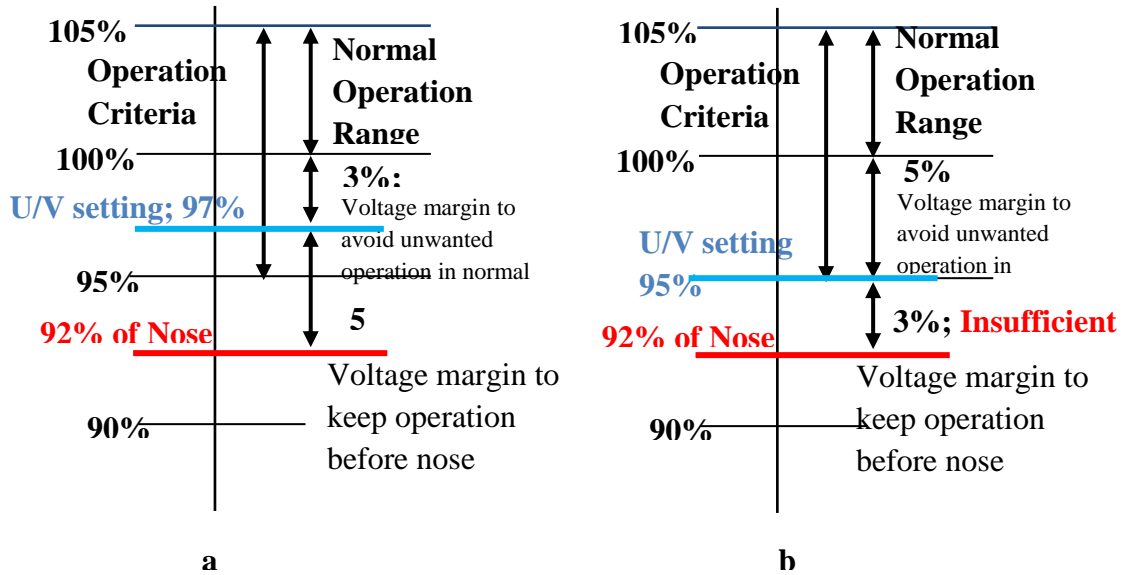


Figure 2.4. Difficulties in Coordinating UVLS Pickup Setting, a) difficulty to keep security (unwanted UVLS responding to normal condition) b) difficulty to keep dependability (Load shedding after system passing nose).

Figure 2.4 illustrates this point. The choice of time delay and the number of set points are also critical settings, especially for distributive or de-centralized schemes which trip load directly. Again, planning studies can provide help in selecting the time and set points. Typically, there are fewer set points in UVLS schemes than are used for UFLS. Some utilities have chosen one voltage pickup point with different time delays for each block of load shed. Time delays are generally set at 2 - 10 seconds— not in the cycle range common for UFLS [5]

Taylor [6] showed the basic concepts for designing under-voltage load shedding, and here are the some of these thoughts:

- In the analysis of voltage stability and under-voltage load shedding design, the characteristic of the load is very important.

- Constant model (power) for the load in steady state study can be sufficient. This case just for the high penetration of motor load, if not, a model take into account voltage dependency should be considered.
- In case there a load area or subarea predominately by motors, UVLS response should be fast to avoid voltage collapse.
- For the load sensitive to the voltage, the under-voltage load shedding scheme is not important, and the voltage can settle down without it.

Based on the mentioned above concepts and others mentioned by the author in his paper

Under voltage load shedding scheme can be as following:

- If the voltage drop to 0.85 p.u., 5 % of the load will be shed with a predetermined time delay (1.5 sec.).
- Shed extra 5% of the load if the voltage 0.87 p.u., with time delay 3 sec.
- Shed another 5% of the load if the voltage 0.87 p.u., with time delay 6 sec.

The above design built on the results of simulations for Puget Sound area utilities and can be generalized, but built a solid ground for under-voltage load shedding program.

Arnborg et al. [22] presented an under-voltage load shedding principle analytically to prevent voltage breakdown. The authors implemented dynamic load modeling. The proposed scheme discussed two approaches of under-voltage load shedding. These strategies named soft and firm and each one has its own advantages [22].

El-Sadek et al. [23] present an optimum load shedding method to avoid voltage collapse. The method adopted risk indicator called Kessel and Glavitsch indicator. The method defines the relation between the amount of load to be curtailed and the indicators

alterations. This is applied for any operation case to decide optimally where and how much load to be shed.

Also Arya et al. [24] developed optimal load shedding scheme taking into account the operation and security of the system. The objective to minimize the load to be shed subject to equality and inequality constraint subjected to voltage stability concerns. Schur indicator is used for the voltage sensitivity. The threshold value for this indicator is used to shed the calculated load. The proposed scheme does two jobs. The first identifies the candidate buses for load shedding with the help of indicator. The second uses differential evolution (DE) undertake the calculation for the amount of load to be shed subject to system security constraints.

Mahari [25]. Proposed an optimal load shedding scheme to prevent voltage collapse. The proposed scheme employs wide area voltage stability index to increase the accuracy of load shedding [25]. The optimal load shedding solves used a Modified version of Discrete Imperialistic Competition Algorithm (DICA). The solution includes all load buses contributing to the load shedding. The scheme gives the location and the amount of load to be shed.

Challenges arise with developing under voltage load shedding are to insure that it operates only for the intended conditions.

The literature survey reveals that the problem of load shedding is addressed usually considering one of two main driving parameters i.e. frequency and voltage. The optimal load shedding in above literature does not address the penetration of the renewable energy



sources into the power system. This thesis develops optimal load shedding taking into account the combined frequency and voltage. It also considers the penetration of renewable energy resources.

## **CHAPTER 3**

### **MODELING AND RESEARCH METHODOLOGY**

#### **3.1 Introduction**

The proposed optimal load shedding in this study is accomplished using MATLAB program with particle swarm optimization algorithm (PSO) for solving the optimization problem. The transient analysis or dynamic analysis before and after load shedding was carried out in Powerworld Simulator. This chapter will explain the procedures and modelling of the system. Also, a brief description of the PSO will be presented.

#### **3.2 Problem Formulation**

The purpose of this study is to minimize network outages. However, curtailing the supply from the consumer is an unfavorable action. Curtailing electrical supply to consumers means a corresponding financial loss to the power companies. It is desirable to minimize the number of consumers who will be subjected to the process of the load shedding. The general requirement is to minimize the amount of load shedding while maintain system security by using available generation reserve.

### 3.2.1 Objective function

The load shedding scheme is formulated as an optimization problem.

$$\min F1 = \sum_{i=1}^N [\alpha_i (P_{Di} - \bar{P}_{Di})^2 + \beta_i (Q_{Di} - \bar{Q}_{Di})^2] \quad (3.1)$$

This function minimizes the load to be shed.

$$\max F2 = \sum_{i=1}^N [c_i (\bar{P}_{Gi} - P_{Gi})^2 + d_i (\bar{Q}_{Gi} - Q_{Gi})^2] \quad (3.2)$$

The second function uses the available generator output reserve.

The two equations can be combined in the following equation

$$\min F = F1 - F2 \quad (3.3)$$

Where

$F$  The objective function for load shedding problem.

$P_{Di}$  and  $Q_{Di}$  The load before load shedding.

$\bar{P}_{Di}$  and  $\bar{Q}_{Di}$  The connected load after load shedding.

$P_{Gi}$  and  $Q_{Gi}$  The generator output at node  $i$  before load shedding.

$\bar{P}_{Gi}$  and  $\bar{Q}_{Gi}$  The generators output at node  $i$  after load shedding.

$\alpha_i, \beta_i, c_i,$  and  $d_i$  Weighting factors.

The above objectives are subjected to the following constraints [17].

### 3.2.2 Generation constraints

$$P_{Gi} = \bar{P}_{Gi} - \frac{P_{Ri}}{R_i} \Delta f \quad (3.4)$$

$$P_{Gi}^{min} \leq P_{Gi} \leq P_{Gi}^{max} \quad (3.5)$$

$$Q_{Gi}^{min} \leq Q_{Gi} \leq Q_{Gi}^{max} \quad (3.6)$$

Where

$P_{Gi}$  The final generation active power at bus  $i$ .

$\bar{P}_{Gi}$  The initial generation at bus  $i$ .

$P_{Ri}$  The rated output of generator.

$R$  The speed regulation.

$f$  The system frequency.

$Q_{Gi}$  The final generation reactive power at bus  $i$ .

### 3.2.3 Load constraints

$$P_{Di} = \bar{P}_{Di} (1 + K_p \Delta f) \left[ p_p + p_c \left( \frac{V_i}{\bar{V}_i} \right)^{N1} + p_z \left( \frac{V_i}{\bar{V}_i} \right)^{N2} \right] \quad (3.7)$$

$$Q_{Di} = \bar{Q}_{Di} (1 + K_p \Delta f) \left[ q_p + q_c \left( \frac{V_i}{\bar{V}_i} \right)^{N1} + q_z \left( \frac{V_i}{\bar{V}_i} \right)^{N2} \right] \quad (3.8)$$

$$P_{Di,min} \leq P_{Di} \leq P_{Di,max} \quad (3.9)$$

$$Q_{Di,min} \leq Q_{Di} \leq Q_{Di,max} \quad (3.10)$$

Where

$\bar{P}_{Di}$  and  $\bar{Q}_{Di}$  The per unit nominal active and reactive power of the load.

$K_p$  and  $K_q$  The load frequency depended coefficient for active and reactive power.

$N1$  and  $N2$  Exponents usually range from 0 to 2 [1].

$p_s$  and  $q_s$  The model parameters that specify the type of the load.

For calculation in the load shedding algorithm, the model takes the value just before disturbance i.e. the nominal value.

### 3.2.4 Load flows equations

$$P_{Gi}(f) - P_{Di}(V, f) - P_i(V, \delta) = 0 \quad (3.11)$$

$$Q_{Gi}(f) - Q_{Di}(V, f) - Q_i(V, \delta) = 0 \quad (3.12)$$

Where

$$P_i(V, \delta) = V_i \sum_{j=1}^N V_j [G_{ij} \cos(\delta_i - \delta_j) + B_{ij} \sin(\delta_i - \delta_j)] \quad (3.13)$$

$$Q_i(V, \delta) = V_i \sum_{j=1}^N V_j [G_{ij} \sin(\delta_i - \delta_j) - B_{ij} \cos(\delta_i - \delta_j)] \quad (3.14)$$

Where

$V_i$  and  $V_j$       The per unit voltage at node  $i$  and  $j$ .

$P$  and  $Q$       The active and reactive power flow.

$G_{ij}$  and  $B_{ij}$       The real and imaginary parts of the line admittance.

$\delta_i$  and  $\delta_j$       Voltage angles at node  $i$  and  $j$ .

*Voltage and frequency constraints*

$$V_i^{min} \leq V_i \leq V_i^{max} \quad (3.15)$$

$$f_{min} \leq f \leq f_{max} \quad (3.16)$$

*Transmission Limits*

$$|\delta_i - \delta_j| \leq \varphi_{ij} \quad (3.17)$$

Where

$\varphi_{ij}$       Angle less than 35 degrees.

The values used in the optimal load shedding are limits whether they are control variables or state variables (will be addressed in the coming sections). Four variables are used to minimize the load and maximize the generation. These variables are called control variables and all are limited as in equation ((3.5, (3.6 and (3.9, (3.10).

### **3.3 System Model**

In this section the models used as test system will be described. There are many system components to choose from. A brief description needs to be given for each component implemented in this study. The parameter values used are given in the Appendix A. The WSCC nine bus system with a three generators and three load buses is used for testing [26]. Also, 39 bus system of New England with 10 generators and 28 load buses is used as a test system [27]. Each generator in the above system has a governor and exciter system besides the modeling of the generator itself will be described in the coming subsection. Loads in the power system have different modelling and the model used in this study will be presented.

#### **3.3.1 Generator model**

The generator used in this study as shown in Figure 3.1 is (Solid Rotor Generator represented by equal mutual inductance rotor modeling) GENROU [28].

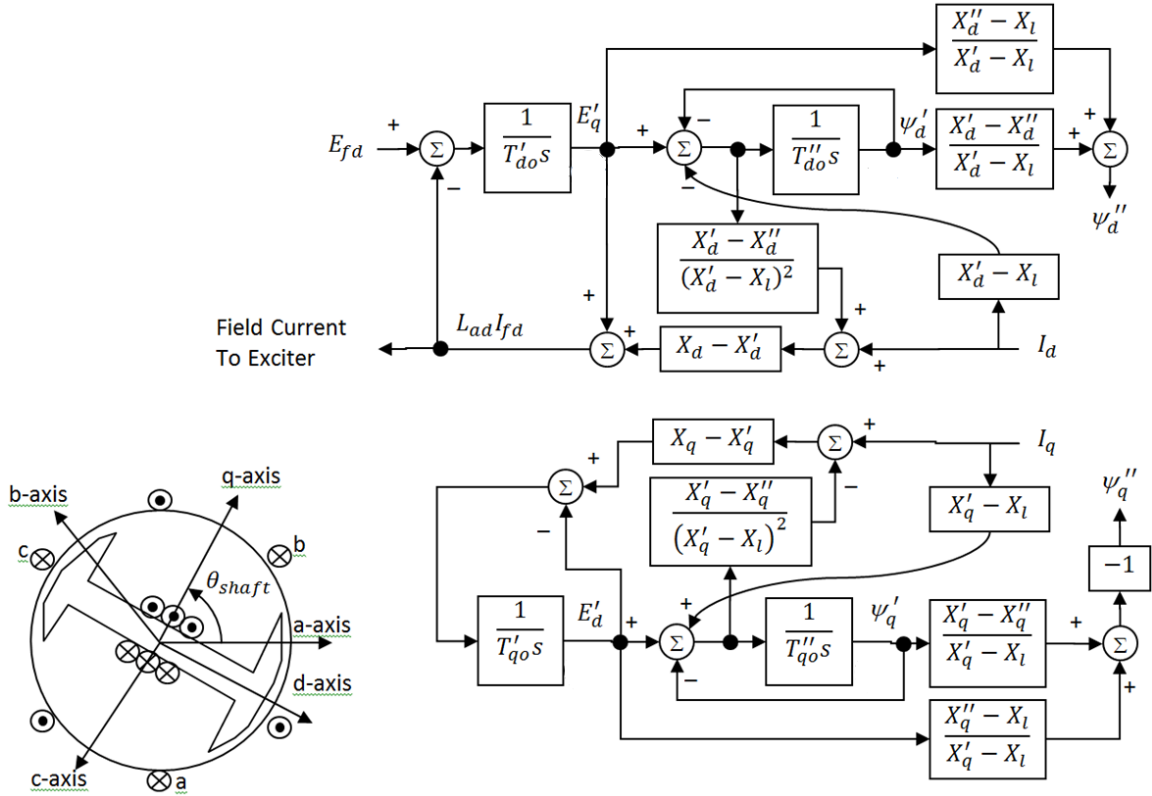


Figure 3.1. GENROU without Saturation [28]

### Mechanical Differential Equations

$$\dot{\delta} = \omega * \omega_0 \quad (3.18)$$

$$\dot{\omega} = \frac{1}{2H} \left( \frac{P_{mech} - D\omega}{1 + \omega} - T_{elec} \right) \quad (3.19)$$

Where

$P_{mech}$  Mechanical input power.

$H$  Generator inertia constant.

$D$  Damping factor.

$\omega$  per unit speed deviation.



$T_{elec}$  Electric torque.

$\omega_0$  Synchronous speed  $2\pi f_0$ .

$f_0$  Nominal frequency.

$$T_{elec} = \psi_d I_q - \psi_q I_d \quad (3.20)$$

$$\psi_q = \psi_q'' - I_q X_d'' \quad (3.21)$$

$$\psi_d = \psi_d'' - I_d X_d'' \quad (3.22)$$

Where

$\psi_d$  and  $\psi_q$  The flux linkages at d-axis and q-axis.

$\psi_d''$  and  $\psi_q''$  The sub-transient flux linkages.

$X_d''$  and  $X_q''$  The sub-transient reactance.

$I_d$  and  $I_q$  The current in  $dq$  axis.

### 3.3.2 Governor model

Power and frequency control in generating units is carried out through governing systems. This processes called load frequency control (LFC). Due to their rotating masses, generating units in power system have stored kinetic energy. This energy is released at the events of the imbalance caused by loss of generation or sudden increased in the load in order to compensate this difference. The kinetic energy stored in the machine is expressed as  $J\alpha = (T_m - T_e)$ , where  $T_m$  and  $T_e$  represent the mechanical and electrical torques respectively,  $J$  represent moment of inertia and  $\alpha$  is rotor angular acceleration [29].

At the start of the disturbance, the mechanical torque is constant. The acceleration factor  $\alpha$  is negative and the rotor start decelerates and the frequency drops due to this events.

The relationship governs the power and the frequency in turbine governor given below

$$\Delta P_m = \Delta P_{ref} - \frac{1}{R} \Delta f \quad (3.23)$$

Where

$\Delta P_m$  Change in turbine mechanical power output

$\Delta P_{ref}$  Change in a reference power setting

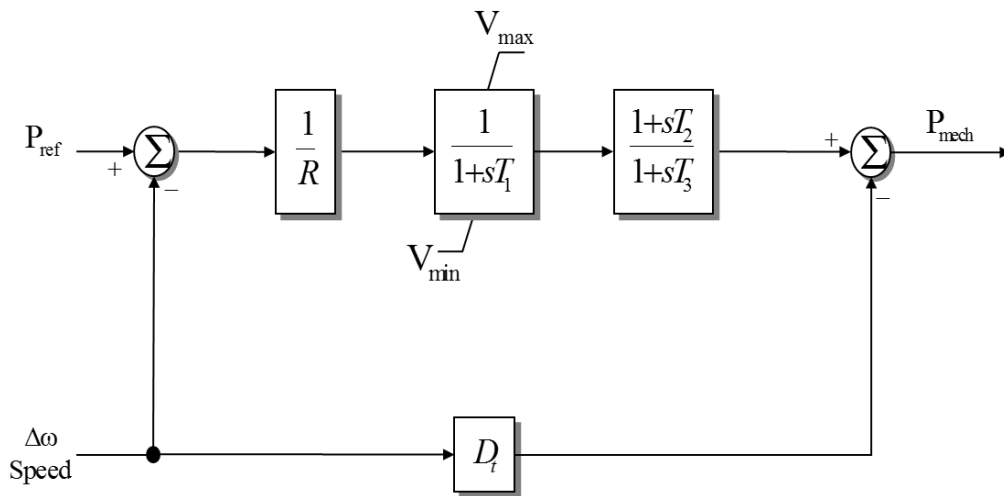


Figure 3.2. Steam Turbine-Governor Model TGOV1

Figure 3.2 shows a schematic diagram of steam turbine governor used in this study [28].

$R$  is the regulation constant,  $\frac{1}{(1 + sT_1)}$  is the time delay associated with the governor  
 $T_2$  and  $T_3$  refer to the reheat and non-reheat time constant,  $D_t$  damping coefficient.  $V_{MAX}$   
and  $V_{MIN}$  are the maximum and minimum valve position limits.

### 3.3.3 Exciter model

The field voltage control is carried out through exciter system which delivers dc power to the rotor winding. The exciter has different types such as a dc generator driven by rotor and this employed with older generators. The static type used by the modern generators. The concept of the static relies on converting ac power to dc through the rectifier. The source of the ac power could be the terminal of the generator or and close bus.

There are many standard block diagram for the exciters (generator-voltage-control) established by IEEE. In this study IEEE Type 1 is used for voltage control. Figure 3.3 shows the block diagram [28].

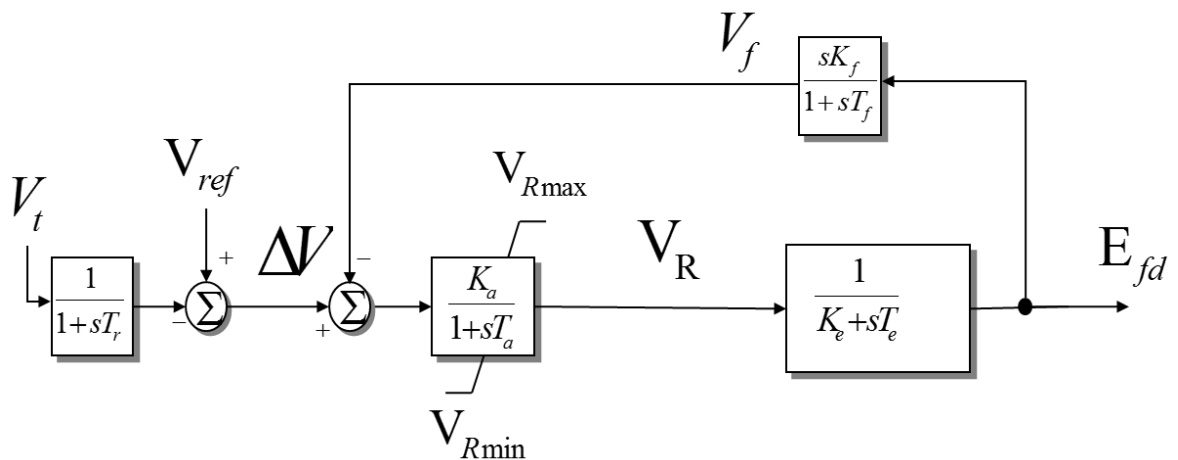


Figure 3.3. Block diagram for IEEE Type 1 exciter.

$\left(\frac{1}{1 + sT_R}\right)$  This is the delay associated with sensed terminal voltage 2 represent  $V_t$ , this value compared to two values, reference value  $V_{ref}$  and value come from the power system stabilizer  $V_s$  if it's utilized in the voltage control. The error  $\Delta V$  sent to voltage regulator. The voltage regulator model is gain  $K_A$  and time constant  $T_A$  which is represent an amplifier the regulated voltage  $V_R$  3 the last stage represent the modeling of exciter dynamic with presence of saturation. 1 Represent the field voltage  $E_{fd}$ . The feedback  $\left(\frac{sK_F}{1 + sT_F}\right)$  is added to improve the dynamic response of the exciter. Lastly, 4 represent the feedback voltage [29].

### 3.3.4 Wind turbine model

The model of the wind turbine depends on the type of the turbine. There are four types of wind turbines named as type1, type2, type3 and type4. Type1 and type2 are modeled as an asynchronous generator. Type3 and type4 are modeled as double fed induction generators (DFIGs). In this study type3 is adopted because it's widely used. A DFIGs is an asynchronous machine which its electrical field fed from rotor and stator. The machine is integrated with the power system network through DC-to-AC converter link the generator with the setup transformer. The representation of DFIG in the transient stability is voltage source converter (SVC) because its dynamics are determined by the converter [29].

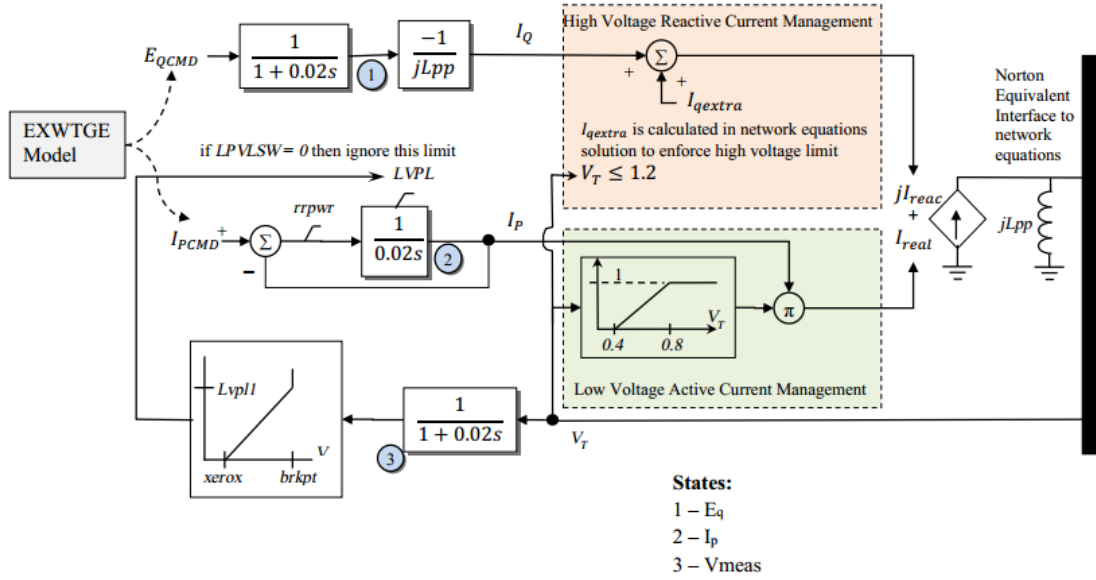


Figure 3.4. Wind turbine model DFAG [28].

The following equations describe the currents injection on the network reference.

$$I_{sorc} = (I_p + jI_q) \quad (3.24)$$

Where

$I_{sorc}$  The injected current to the network which is combination of current

$I_p$  The in phase current with terminal voltage and

$I_q$  The reactive power current which can be controlled as seen in Figure 3.4.

The reactive voltage  $E_q$  is driven by the following equation

$$E_q = -I_q X_{eq} \quad (3-25)$$

Where

$X_{eq}$  Effective reactance that keep the current  $I_p$  in phase with terminal voltage.

### 3.3.5 Load modelling

The model of the load in power system has different types. For the power system stability study purposes, it's preferable to represent the load as a composite load. Generally, the load is divided into two groups: Static and dynamic loads.

#### *Static load*

Static load deals with the characteristic of the load as an algebraic function of frequency and the bus voltage that the load connected to. Mathematically this load has two representation.

#### *The exponentially model*

$$P_{Di} = \bar{P}_{Di}(\bar{V})^a(1 + K_p\Delta f) \quad (3.26)$$

$$Q_{Di} = \bar{Q}_{Di}(\bar{V})^b(1 + K_q\Delta f) \quad (3.27)$$

Where

$\bar{V}$       The per unit voltage.

$P_{Di}$      The active part of the load.

$Q_{Di}$      Reactive part of the load.

$K_p$  and  $K_q$      The load frequency depended coefficient for active and reactive power.

$a$  and  $b$          Exponents usually range from 0 to 2 [1].

#### *The polynomial model*

$$P_{Di} = \bar{P}_{Di}(1 + K_{pf}\Delta f)[p_p + p_c(\bar{V})^{N1} + p_z(\bar{V})^{N2}] \quad (3.28)$$

$$Q_{Di} = \bar{Q}_{Di}(1 + K_{qf}\Delta f)[q_p + q_c(\bar{V})^{N1} + q_z(\bar{V})^{N2}] \quad (3.29)$$

Where

$p_s$  and  $q_s$  The model parameters that specify the type of the load.

### Dynamic load modelling

The dynamic loads include motors and discharged lighting load and many others. A complex load (CLOD) representation to include this feature is used as shown in Figure 3.5.

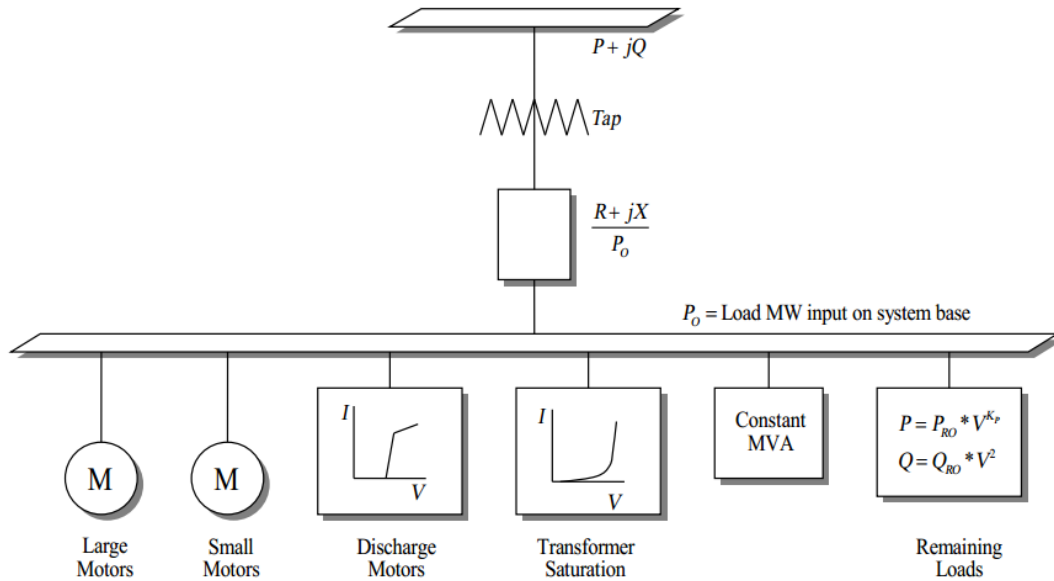


Figure 3.5. Load Characteristics CLOD [28].

### 3.4 Optimization Methods

Most of the optimization problems seek to either minimize or maximize a desired objective function. The solutions of the objective function can be limited by boundaries. These boundaries are referred to by inequality constraints. The control parameters (should be linearly independent parameters) which are used to get the minimum or maximum of the objective are required to achieve equality constraints.

The optimization process can be summarized in the following steps.

- Specify the parameters that will be used in the design.
- State the constraint clearly and formulated.
- Write the equation of the objective function in a way that serves your design
- Set the boundary for the feasible solution.
- Pick a suitable optimization technique to solve your problem
- The last step solves to get you optimal values.

Generally, the formulation of any optimization problem is stated as follows:

$$\text{Minimize } F(x) \tag{3.30}$$

Subject to

$$G(x) = 0 \tag{3.31}$$

$$H(x) \leq 0 \tag{3.32}$$



Where  $G(x)$  the equality and  $H(x)$  inequality constraints.

The control variables in the optimization problem have a big share in the output nature. And the procedures for selecting these variables are not an easy job, and how to identify which variable has more effect on the solution than other especially in some optimization techniques will be discussed in the coming paragraphs. The decision variable is categorized as control flow logic. The space of the feasible solution is limited by the constraints set it to the problem.

The problem of optimal load shedding is similar to the optimal load flow problem. The same optimization techniques that used with optimal load flow can suit the optimal load shedding because the constraints almost same for the both problem.

In general, the mathematical programming is the nonlinear programming problem. For more details about the nonlinear programming, methods refer to [30].

In practical engineering design optimization, the difficult part experienced is the part of handling constraints. When we deal with the problems of the real world, often the constraints that we are exposed to non-linear and nontrivial in terms of engineering design [30]. The feasible solutions often limited by the constraints which determine the solution domain.

The nature of the constraints is complex and unusual, and this makes a deterministic solution impossible. Many evolutionary algorithms have been proposed lately for constrained engineering optimization problem beside the methods of handling constraints. The core part of the optimization procedure [30].

Heuristic algorithms for Evolutionary programming and genetic algorithm (GA) have been adopted lately in solving optimal power flow problem. The outcomes described were encouraging and empowering for more research in this area [31]. There has been a deficiency relate to the use of GA in this area discovered by a researcher, especially when the parameter being optimized are highly correlated.

A new evolution computation technique has been proposed by Kennedy & Eberhart 1995 [32] named Particle Swarms Optimization (PSO). Generally (PSO) in its principle is simple, easy-to-representation, and efficient computationally. In this research, the PSO is used to solve the optimization problem.

### 3.4.1 Basic fundamentals of PSO algorithm

In the following points, the important basics of the particle swarm technique are listed and cleared [30],[31]

- i. *Particle*  $X(t)$ : An n-dimensional real value vector nominee, where n is the optimized parameters number. At time k, the  $i$ th particle  $X(k, i)$  state it as follow

$$X_i(k) = [X_{i,1}(k); X_{i,2}(k); \dots; X_{i,m}(k); \dots \dots; X_{i,d}(k)] \quad (3.33)$$

Where

$X_s$  Parameters to be optimized

$X_n(k, i)$  The nth optimal parameter in the  $i$ th nominee solution

$d$  the number of control variables

- ii. *Population*: This is a group of m vector (particles) at time  $k$ ,  $pop(k)$ .

And it is as follow:

$$pop(k) = [X_1(k), \dots, X_m(k)]^T \quad (3.34)$$

iii. *Swarm*: This is randomly generated population of moving particles that incline to assembly together and every particle appears to be swimming in an irregular route.

iv. *Particle velocity  $V(t)$* : In a n-dimensional real value vector nominee each particle  $i$ th have a velocity in each time  $k$ ,  $V_i(k)$  can be defined as

$$V_i(k) = [v_{i,1}(k); v_{i,2}(k); \dots; v_{i,n}(k); \dots \dots; v_{i,d}(k)] \quad (3.35)$$

Where

$v_{i,m}(k)$  The velocity of the  $i$ th particle with reverence to the  $m$ th dimension.

v. *Individual best  $X^*(t)$* : During the movement of particles in the domain of search, the algorithm compares the objective function value at the present position with the last minimum stored value for the objective which is obtained previously and stored. The position related to this value is identified as individual best and labeled by  $X^*(k)$  . This value is updated for each particle swarm during the investigation process. The expression for the individual is defined as follow

$$X_i^*(k) = [x_{i,1}^*(k), x_{i,2}^*(k), \dots, x_{i,d}^*(k)]^T \quad (3.36)$$

The individual best of the  $j$ th particle in minimizing one objective function f,

$X_i^*(k)$  is updated whenever  $f(X_i^*(k)) < f(X_i^*(k - 1))$ .

- vi. *Global best  $X^{**}(t)$* : Among the majority of the individual best positions accomplished up to this point this the best position.

The particle swarm optimization is unconstrained optimization technique, and there are many ways used to handle the constraints. The most famous handling technique is penalty function. In this study, the problem of constraints handling is handled by generating feasible solution. This way we guarantee a solution with all constraints is preserved.

Figure 3.6 shows the flow chart for PSO algorithm.

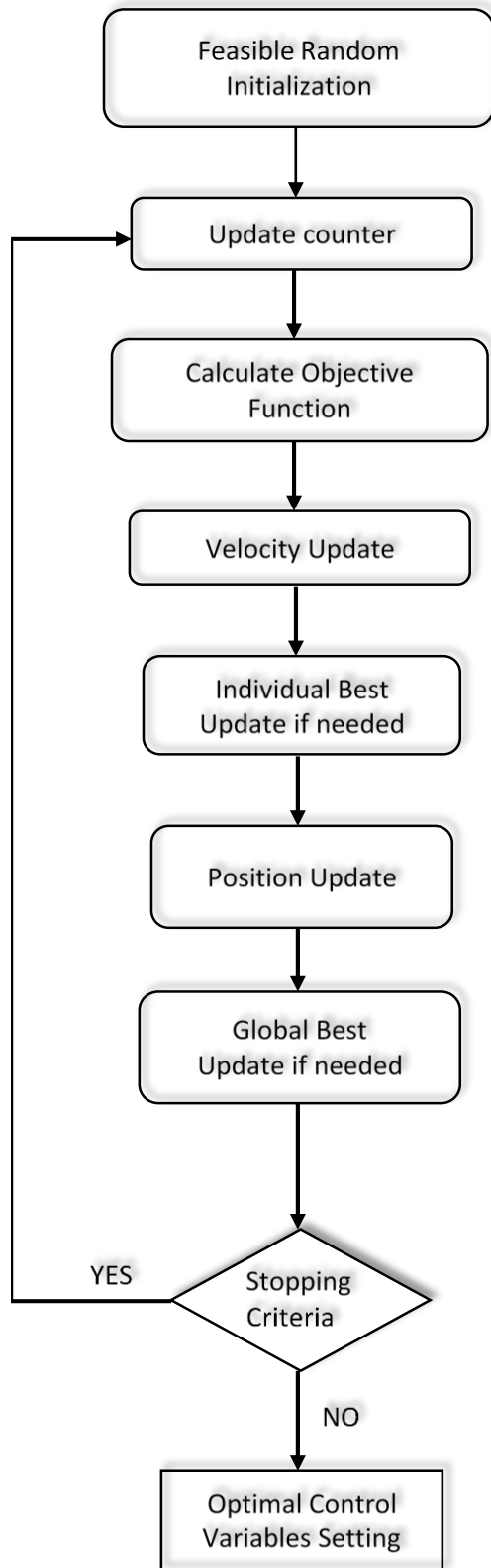


Figure 3.6. The algorithm for PSO

### 3.5 The procedure for load shedding

Figure 3.7 shows the overall diagram for the optimal load shedding process.

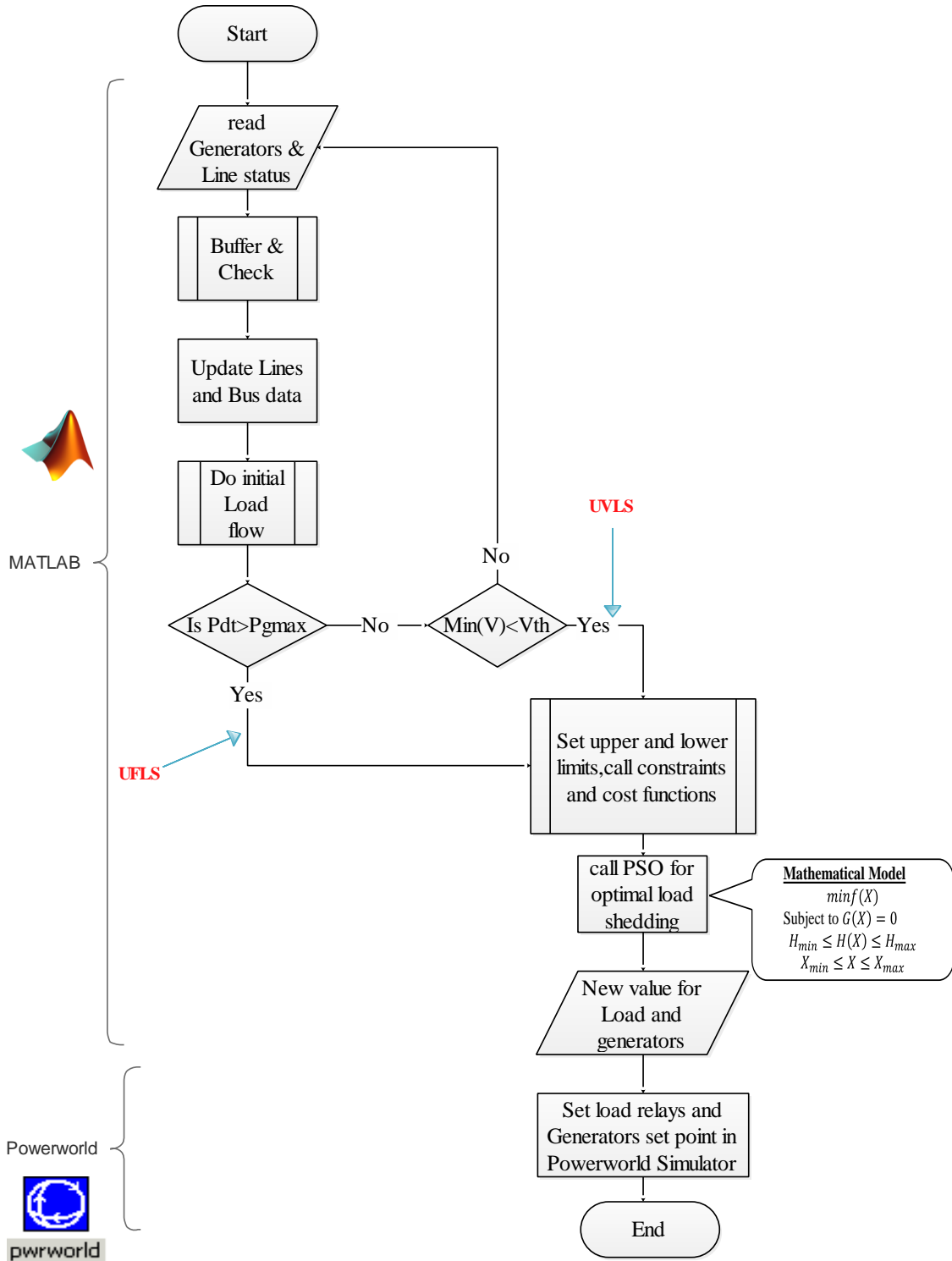


Figure 3.7. Optimal load shedding diagram

The following points elaborate the load shedding process.

- The program starts by reading the online generators data and the line status (connected or disconnected).
- These values will pass through a buffer. The buffer is a comparator which compares all generators output values with reference saved value inside the program and makes any necessary change like chose new slack bus if the slack generator out of service or changes the limit value for the generator encounter a problem, and the output is reduced.
- If any change is required in the previous step, the values of the bus data and line data will be updated to the new setting.
- An initial load flow will be conducted to update the bus voltage and generation output.
- From the results of the load flow, two components will be examined, the total load compared to the available generation and reserve. This test for the under frequency event.
- If the load exceeds the generation plus reserve, control action will be issued to calculate the new system stable points based on load flow. The program will set the minimum and maximum value according to pre-saved values for the system and calls the objective function constraint files with the help of PSO to calculate the new load and generation of the system.
- The output of the optimization algorithm will be passed again to the bus data to update the load and generation values.

- As last steps of the MATLAB program, the load flow will be carried out to make sure the value of the voltage and angle within the specified limits.
- All steps mentioned before will be followed if the case is a voltage drop below permissible values.

The program is tested on two power system to validate the proposed scheme: *WECC 9\_bus\_system* and *IEEE\_39\_bus system*, the two test systems are built in Powerworld Simulator for dynamic analysis.



# CHAPTER 4

## RESULTS AND DISCUSSION

The main purpose of optimal load shedding is to minimize the outages due to disturbances in the networks. In this chapter, the results obtained from applying the load shedding scheme on 9-bus system [26] and 39-bus system [27] will be introduced. Weighted factors for the objective function were taken as unity. Also, results due to conventional load shedding will be presented for the sake of comparison.

### 4.1 Study system 1: WECC 9 bus system

The proposed optimal load shedding scheme is first tested on a WECC 9-bus, 3-machine system that is illustrated in [31]. Its diagram is shown in Figure 4.1.

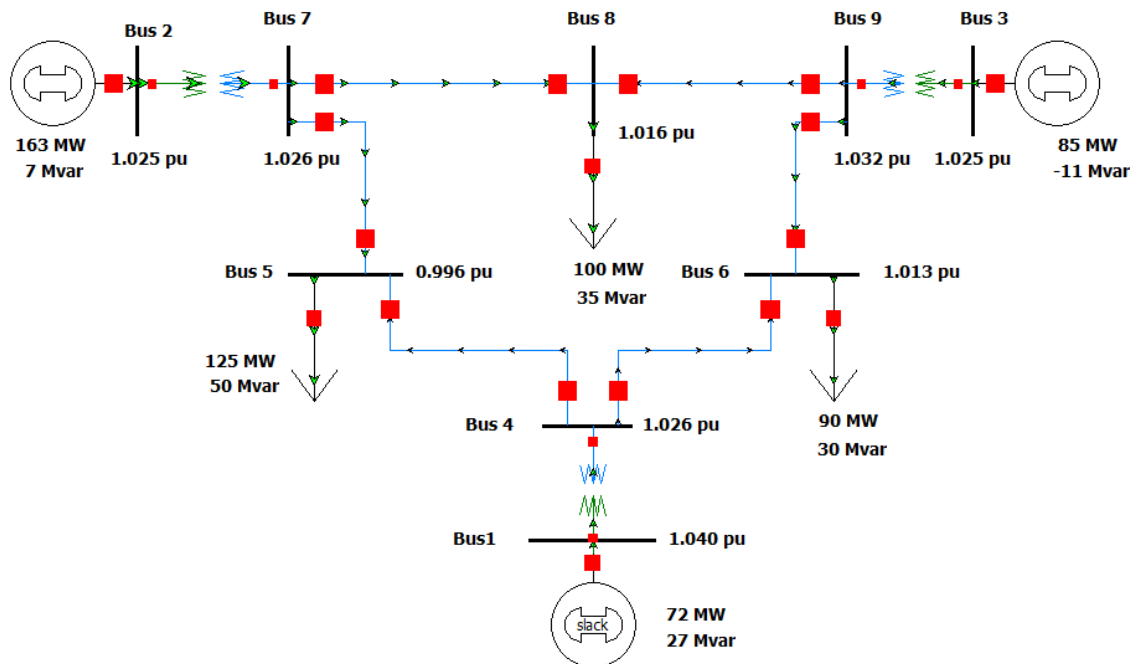
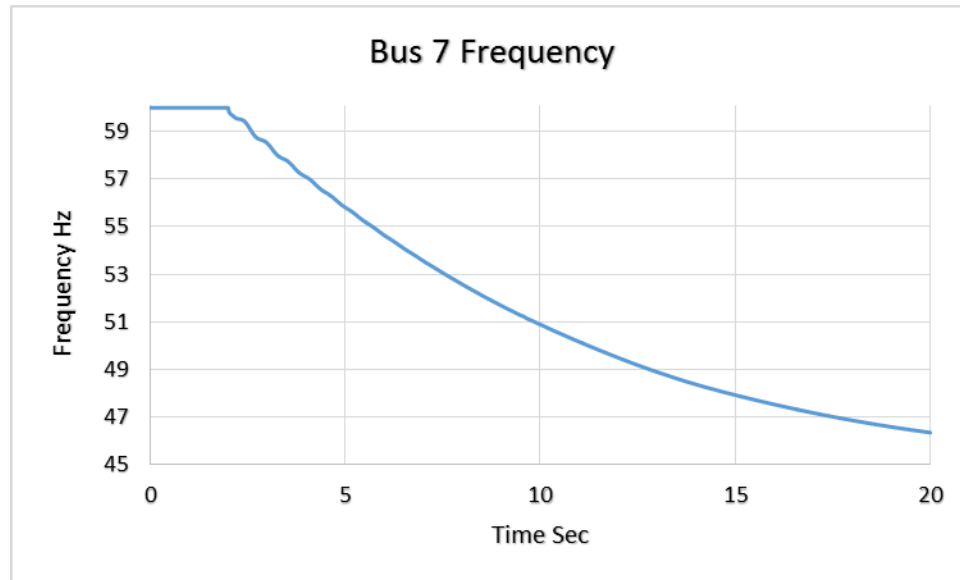


Figure 4.1. WSCC 9 bus test system

The first disturbance is that generator 2 with a generation capacity of 163 MW is out of service for a period of 2 seconds. Figure 4.2 shows the frequency response at bus number 7 without load shedding. The maximum capacity for the other two generators is set to 150 MW.



**Figure 4.2 Frequency response without load shedding**

The frequency declines to 46 Hz in 19 second due to loss of generator 2 (Figure 4.2). The operation at this level of frequency is unfavorable because it could result in high magnetizing currents in transformers and induction motors. Moreover, speed-based applications such as valves, protection device etc. will be impacted

The following sections will present the solution for frequency decay using two load shedding schemes i.e. conventional load shedding scheme and optimal load shedding scheme.

### 4.1.1 Conventional load shedding

In conventional under frequency load shedding, the relays in the substation at the load areas drop specific amount of loads at predetermined low frequency [33].

Table 4.1 shows the setting of the load relays as taken from reference [1].

Table 4.1. Conventional load shedding setting

Frequency Threshold	Time Delay Sec.	Breaker Time Sec	Percentage load Shed % S
59.5	0.2	0.1	10%
59	0.2	0.1	15%
58.8	0.2	0.1	25%

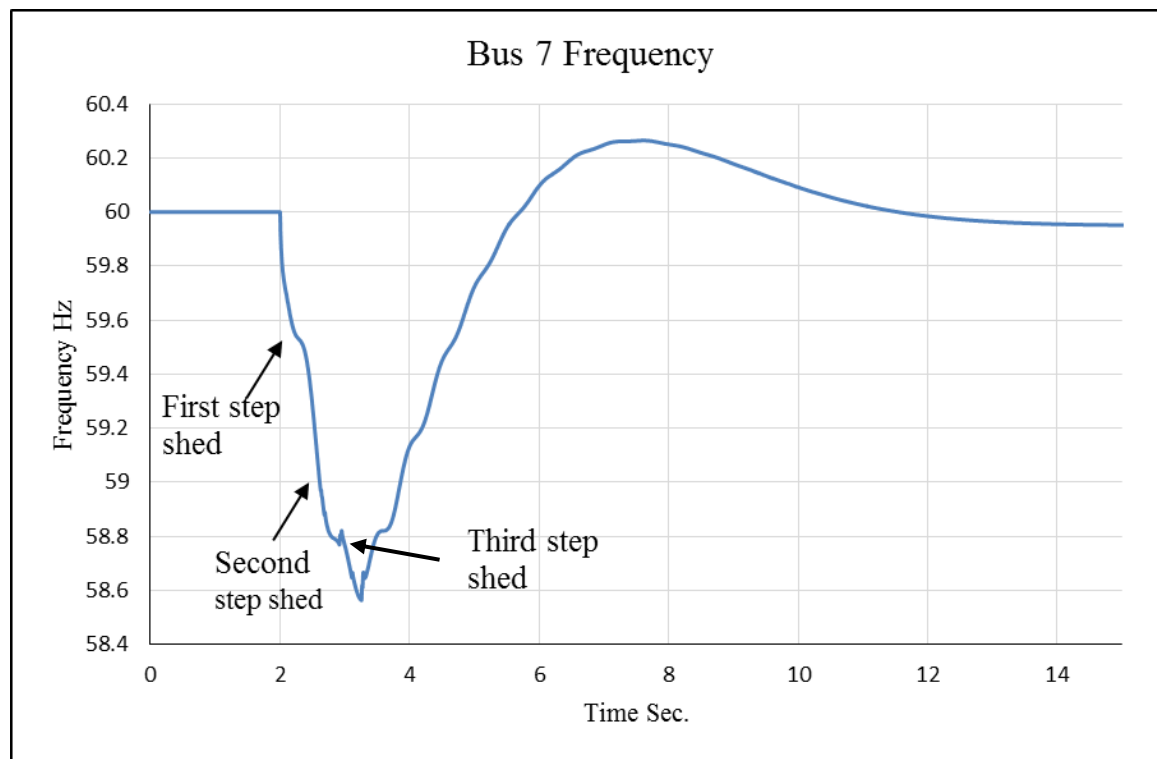
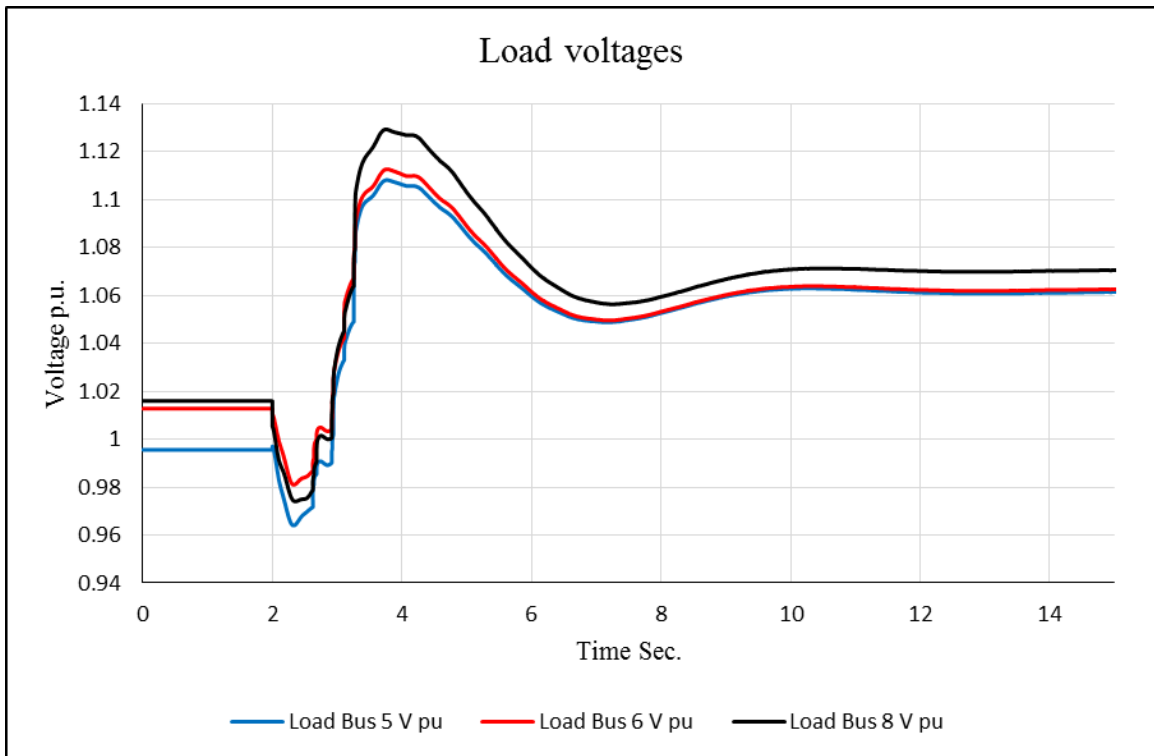


Figure 4.3 Frequency response due to conventional load shedding

Due to conventional load shedding the frequency drop to 58.5 Hz after 50 % of the load is dropped as shown in Table 4.1. It starts rising again with overshoot 0.25 Hz and finally settles around 60 Hz after 9 seconds of the beginning of the load shedding as shown in Figure 4.3.

The problem with this conventional load shedding it can reach a critical level or even exceeds the threshold value of the protection relay and initiates unwanted protection actions. Also, the value of the voltage at bus can exceed the operation limits because the load shedding process is based on stopping the frequency decline without considering another stability issue that can emerge due to the load shedding process. Figure 4.4 shows the voltages at load buses after load shedding. The value of the voltage at all load buses is above 1.05 p.u. (1.06-1.07) which violates the operating limit for this system.



**Figure 4.4** Voltages at load bus after conventional load shedding

### 4.1.2 Optimal load shedding with reserve

In this scenario, the proposed optimal load shedding considers that generators do not operate at the full capacity limit. Thus there is room to increase (reserve) generation. The bus data output for the system in healthy condition is shown in Table 4.2. After the disturbance, the program calculates the load to be shed and the corresponding generation is the bus data is updated in Table 4.3

**Table 4.2 Bus output data for a healthy IEEE 9 bus system**

Bus	Type	V (p.u.)	Angele (degrees)	PG (MW)	QG (MVAR)	PL (MW)	QL (MVAR)
1	swing	1.04	0	71.645	27.408	-	-
2	constant voltage	1.025	9.285	163	7.033	-	-
3	constant voltage	1.025	4.671	85	-10.071	-	-
4	Load	1.026	-2.217	-	-	-	-
5	Load	0.996	-3.99	-	-	125	50
6	Load	1.013	-3.687	-	-	90	30
7	Load	1.026	3.723	-	-	-	-
8	Load	1.016	0.731	-	-	100	35
9	Load	1.032	1.972	-	-	-	-
Total				319.645	24	315	115

\*base MVA=100 MVA,  $V_{base}$  =16.5Kv, 18Kv and 13.8Kv at buses 1, 2 and 3 respectively and 315Kv for the rest buses.

**Table 4.3 Bus output data for IEEE 9 bus system after loss generator 2 and shedding scheme work.**

Bu s	Type	V (p.u.)	Angele (degrees)	PG (MW)	QG (MVAR)	PL (MW)	QL (MVAR)
1	swing	1.04	0	134.88 7	22.793	-	-
2	constant voltage	1.022	-7.936	0	0	-	-
3	constant voltage	1.025	2.054	135	-7.072	-	-
4	Load	1.03	-4.159	-	-	-	-
5	Load	1.004	-8.715	-	-	109	49
6	Load	1.019	-5.876	-	-	74	30
7	Load	1.022	-7.936	-	-	-	-

8	Load	1.013	-7.448	-	-	84	35
9	Load	1.032	-2.235	-	-	-	-
		Total		269.88	15.722	267	114
		Percentage shed				15.24%	0.87%

The load relays setting in Powerworld simulator are shown in Table 4.4.

Table 4.4. Optimal Under frequency load shedding -- Frequency Threshold—59.6.

Load Buses	Time Delay Sec.	Breaker Time Sec	% MW Shed	% MVAR Shed
Bus 5	0.2	0.1	12.8%	2%
Bus 6	0.2	0.1	17.78%	0%
Bus 8	0.2	0.1	16%	0%

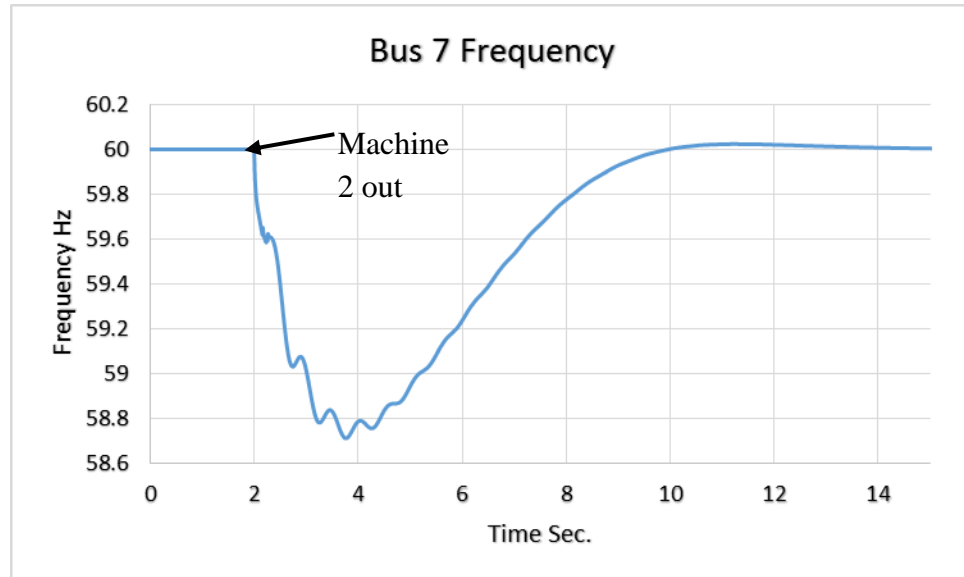


Figure 4.5 Frequency response at bus 7 for load shedding with reserve

Figure 4.5 shows that the frequency dropping to 58.75 Hz after load shedding scheme was engaged (pick up frequency 59.6), and dropped the calculated amount of load to be shed

as shown in Table 4.4. The frequency settles at the nominal value after 8 seconds when shedding started.

Figure 4.6 shows the voltage at load bus after load shedding. The values show that all the specified voltage limits at the load shedding process were met.

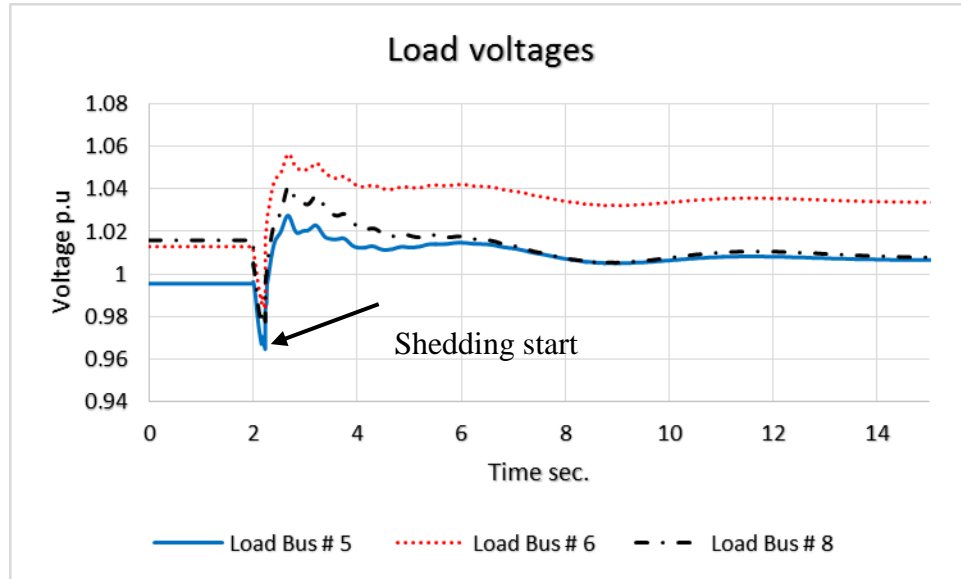


Figure 4.6 Voltages at load buses after load shedding

Figure 4.7 shows a comparison between the frequencies response at each case discussed above. The limits lines in the graph indicate a trip zone of generators. The nearest curve from these zone is the frequency curve due to conventional load shedding. For optimal load shedding, the frequency decline stops after a few seconds from the shedding start, before the frequency hit 59 Hz. This makes the proposed optimal load shedding very effective in stopping the frequency decline.

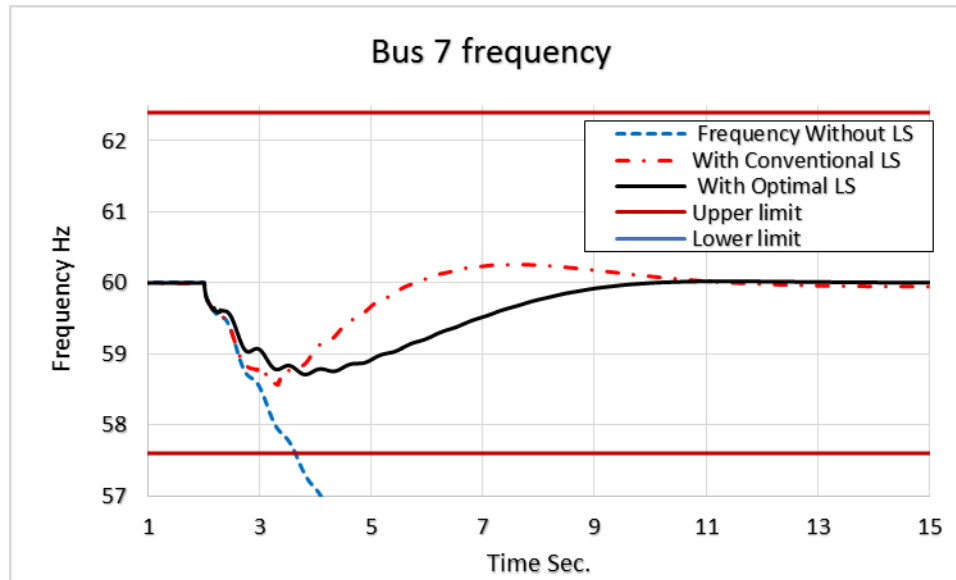


Figure 4.7. Comparison between frequencies at each case

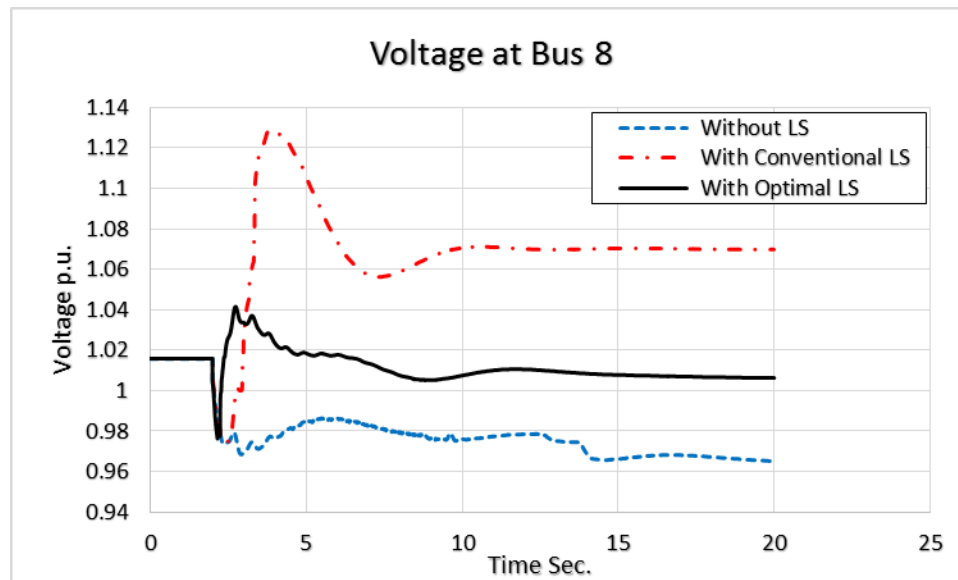
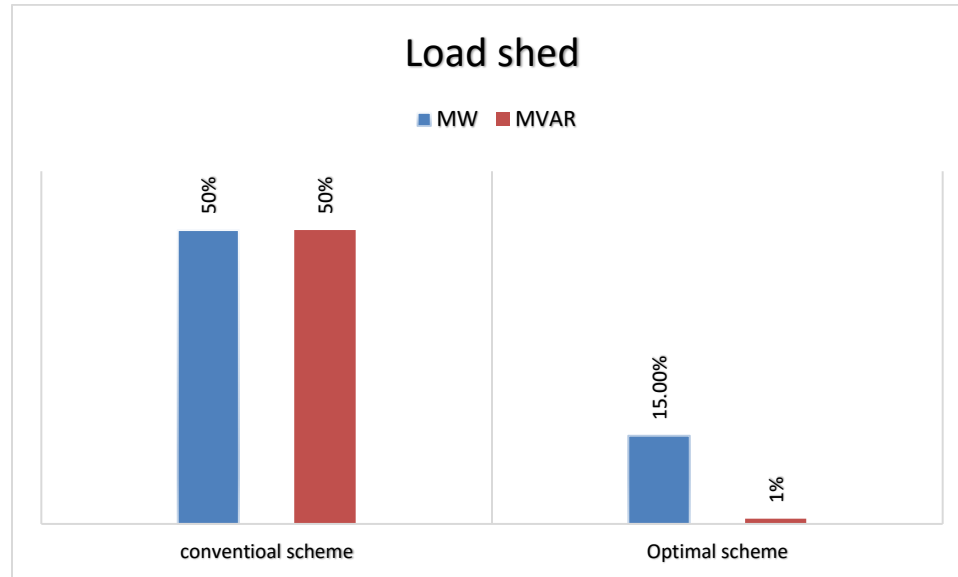


Figure 4.8. Voltage at load bus 8 in all cases

Figure 4.8 compares the value of the voltage at load bus 8 for all previous cases. The dotted line for the voltage without load shedding, dash-dot line for voltage value with conventional load shedding, smooth line indicates the voltage with optimal load shedding. The voltage at bus 8 violates the upper limits for the conventional load shedding scheme.



The bar chart below compares the values of the load that shed in each load shedding technique.



**Figure 4.9. Total load shed in each load shedding scheme**

The optimal load shedding scheme shed 70% less load compared to the conventional load shedding scheme. The conventional scheme shed the same amount of active and reactive power as shown in Table 4.1. Whereas the optimal scheme deals with active and reactive power separately. It takes into consideration the voltage limit in load shedding process. The optimal scheme shed less load in order to restore the frequency to its operating level.

### **4.1.3 Comparison with published work on optimal load shedding**

In this section, a comparison of the proposed scheme with another scheme done by Xu 2001 [34] is presented. Table 4.5 shows the algorithm used in each scheme and the generation limit adopted in each model. The case of comparison is that generator 2 in WSCC 9 bus system loss 100 MW.

**Table 4.5 Comparison between two optimal load shedding schemes when generator 2 loss 100 MW**

Base case			After load shedding					
			Using proposed work Algorithm : PSO			The compared with work [34] Algorithm: non-linear programing		
Bus	PG (MW)	PL (MW)	PL (MW)	Min Gen.(MW)	Max Gen. (MW)	PL (MW)	Min Gen. (MW)	Max Gen. (MW)
1	71.645	-	-	0	200	-	0	200
2	163	-	-	0	200	-	0	200
3	85	-	-	0	200	-	0	200
4	-	-	-	-	-	-	-	-
5	-	125	112	-	-	106.7	-	-
6	-	90	76	-	-	90	-	-
7	-	-	-	-	-	-	-	-
8	-	100	100	-	-	44.13	-	-
9	-	-	-	-	-	-	-	-
Total percentage (MW )shed			8.75%			23.55%		

\*Min and Max generations in this comparison refer to the margin of generators output used with algorithms during calculate the load to be shed

The total load shed using the proposed load shedding scheme is less than the other scheme [34] as shown in table 4.5. The result shows the effectiveness of the proposed scheme.

#### **4.1.4 Loss of transmission line 4-5 in WECC 9 bus system**

In this section, the results of loss of transmission line 4-5 in 9 bus system will be presented. Figure 4.10 shows the effect of loss transmission line on load voltage. The voltage drop to 0.86 p.u. and settle at 0.89 p.u. and correction action needs to be carried out.

Figure 4.11 shows the frequency response at bus 7. The graph shows that the frequency is rising above 60 Hz and settle at about 60.1 Hz. This value acceptable in term of frequency stability.

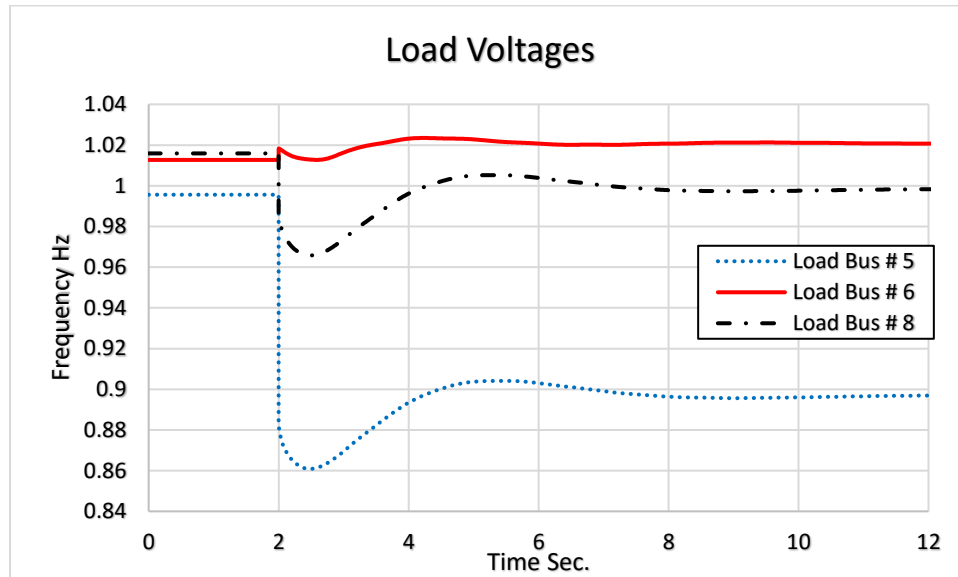


Figure 4.10. Load voltage after loss line 4-5

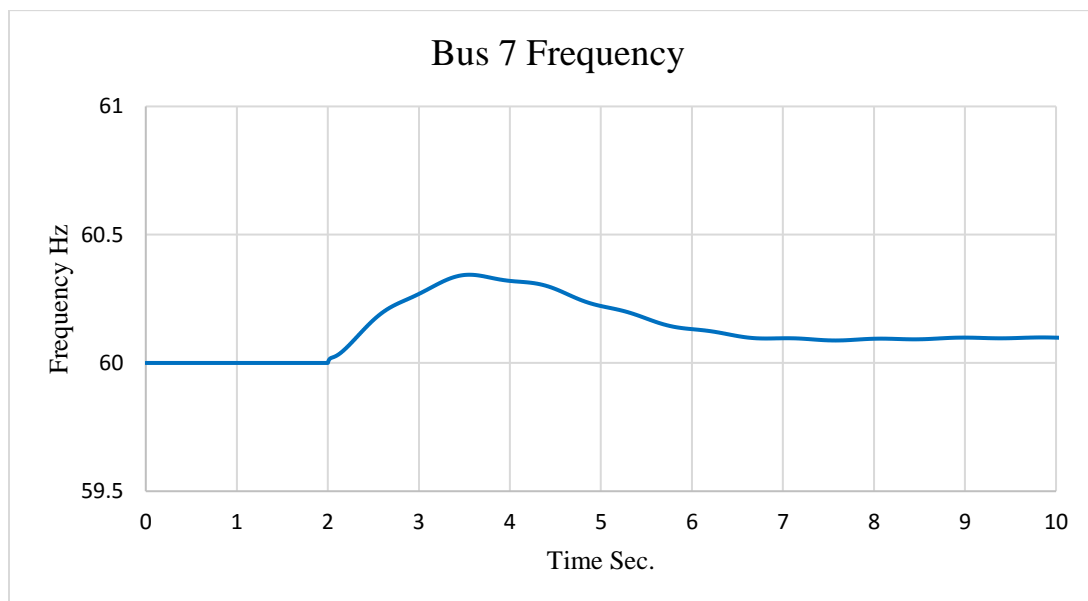


Figure 4.11. Frequency response after loss of transmission line

The results from the optimal load shedding program suggest shedding 43 MVAR from bus 5 to regain stable operation state of the system. Figure 4.12 and Figure 4.13 give the status of the voltage at load buses and frequency of the system respectively after load shedding. The figures validate the expected results from the optimizer and voltage at bus 5 is back to the safety operation level.

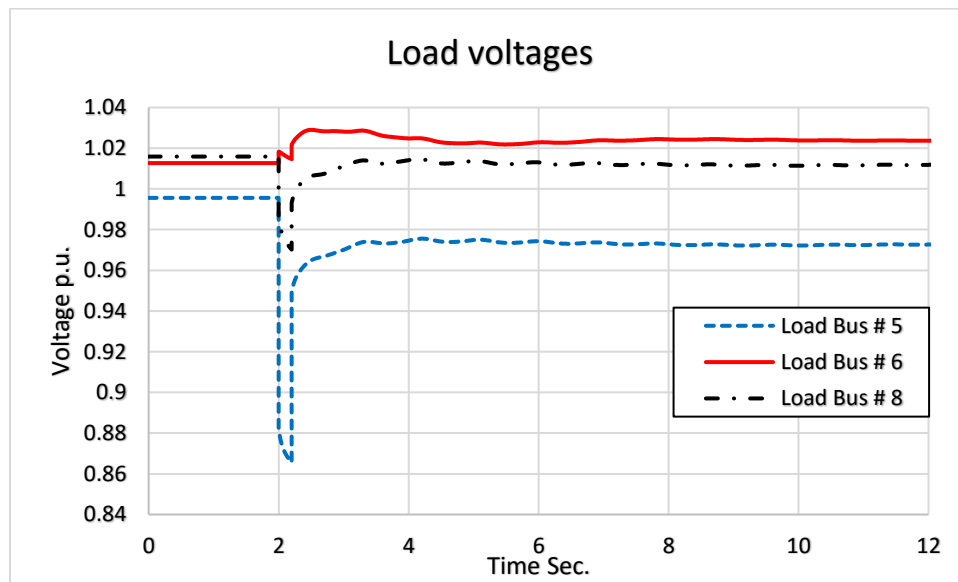
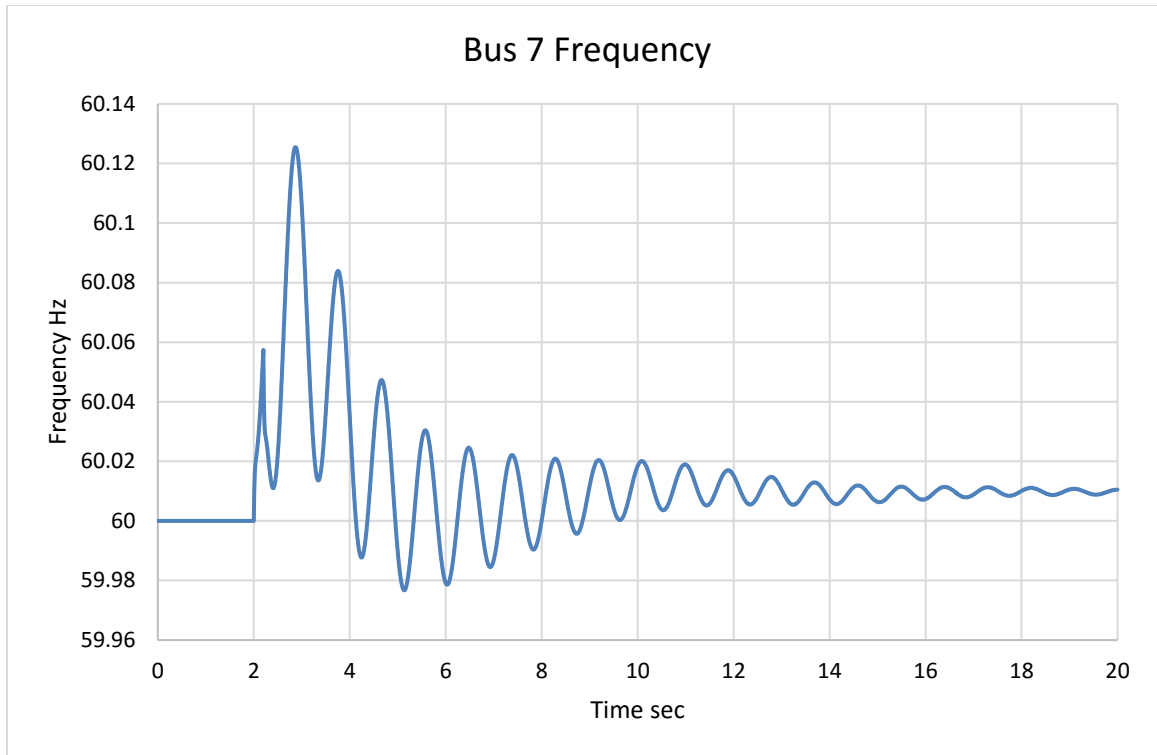


Figure 4.12. Load voltages after load shedding

The frequency oscillates after load shedding between 60.04 Hz and 59.98Hz and finally damped to 60.01 Hz as shown in Figure 4.13.



**Figure 4.13. Frequency response at bus 7 after load shedding**

## **4.2 Study system of WECC 9 bus in the presence of wind turbine.**

Wind plants have restricted capability to control active power. Under ordinary conditions, the objective is to extract as much energy from the wind. Electrical disturbances create a temporary imbalance between the electrical and mechanical power. How this discrepancy is handled depends on the type of Wind turbine generators (WTGs) and how they are controlled.

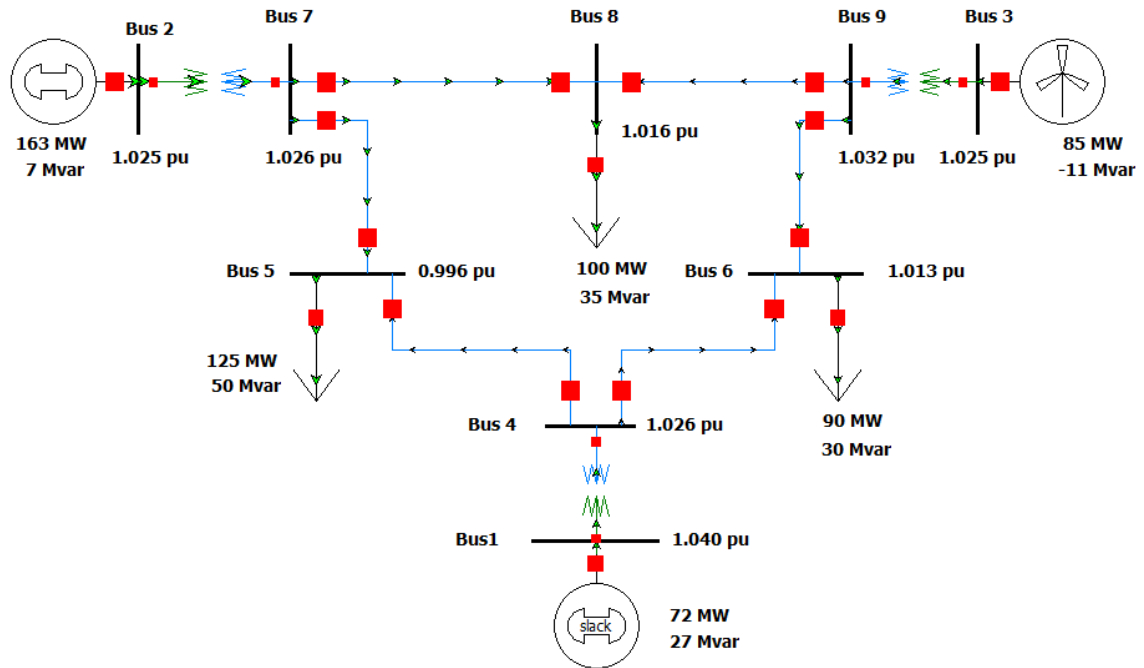


Figure 4.14. WSCC 9 bus system with wind turbine

Type-1 and Type-2 WTGs are directly connected to the grid; they provide a small amount of inertial response. Type-3 and Type-4 WTGs do not inherently have an inertial response because their generators are effectively isolated from the grid by the converter dynamics.

The existing WECC generic dynamic model implementation assumes that the wind speed is constant during the typical dynamic simulation run (10 to 30 seconds). The dynamics associated with a change in the wind power are not considered [35].

Figure 4.14 shows the 9 bus test system where generator 3 with 85 MW loading will be replaced with wind turbine with the same size. The purpose of this study is to investigate the effect of the presence of wind turbine in power system on load shedding. For the sake of simplicity, just two scenarios will be presented, Conventional and optimal load shedding schemes.

The effect of integrating the wind to the power system in term of frequency response can be seen in Figure 4.15. The curve of the frequency in case of wind is steeper than the one for conventional generation. This is because the presence of the wind will reduce the rotating mass in the system therefore the rate of change of frequency will be large.

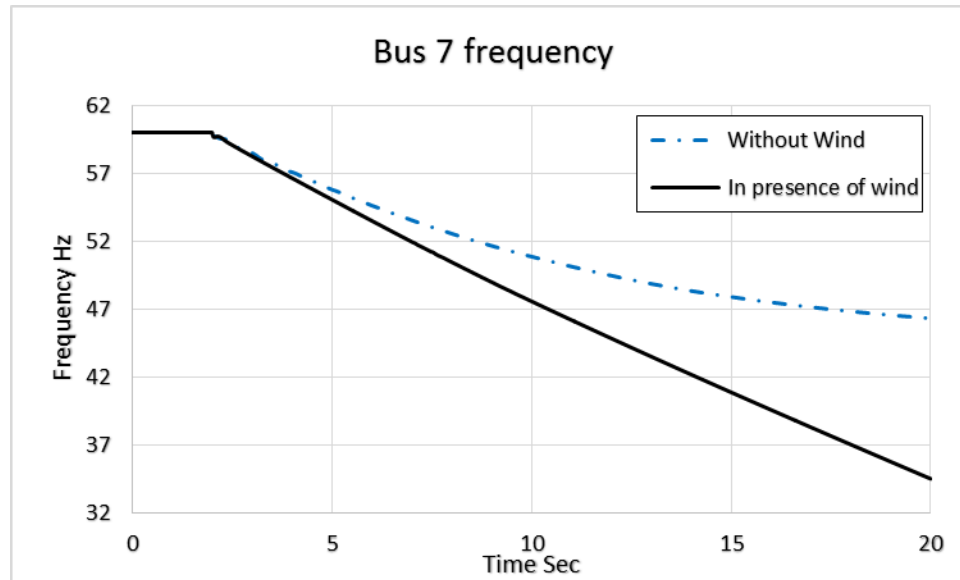


**Figure 4.15. Frequency response in the presence of wind**

The following sections will present the solution for frequency declines using two load shedding schemes i.e. conventional load shedding scheme and optimal load shedding schemes.

#### **4.2.1 Conventional load shedding.**

Here the conventional load shedding on the system in the presence of wind is presented in Figure 4.16

The same setting for conventional load shedding used in Table 4.1 is deployed in this case.

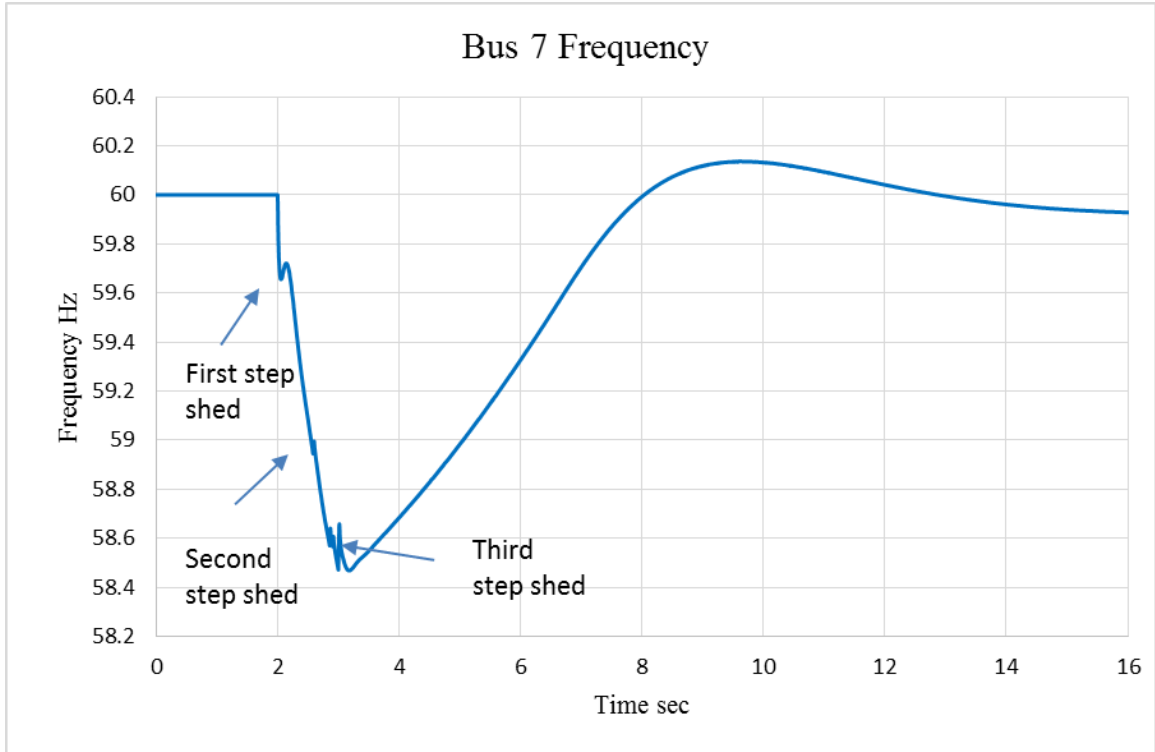


**Figure 4.16. Frequency response in conventional load shedding**

The frequency depicted in (Figure 4.16) drops to 58.5 Hz after load shedding is initiated. The frequency rises to 60.15Hz i.e. with 0.15Hz overshoot and settle around 60Hz after 11 seconds from the beginning of load shedding.

The voltage on the load buses after load shedding is shown in Figure 4.17. The values of voltages in all load buses are higher than the operation levels. Voltages at bus 5 and 6 are stabilized at 1.08 p.u. after 2 seconds from load shedding whereas the voltage at bus 8 reaches 1.1 p.u. after 4 seconds from load shedding and both values are violations.



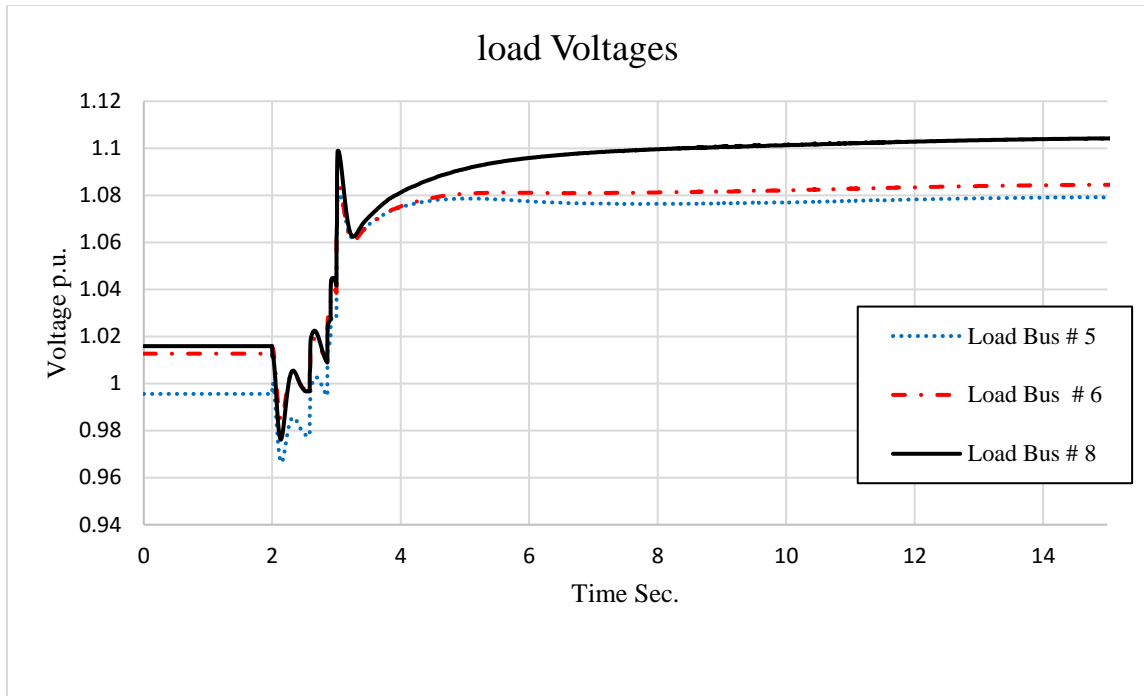


Figure 4.17. Load voltages after load shedding

#### 4.2.2 Optimal load shedding with reserve

The amount of load shed due to loss generator 2 in the presence of wind turbine is more than the load shed when no wind turbines were included (Table 4.6 & Table 4.4).

Table 4.6 Bus output data for WECC 9 bus system after loss generator 2 and shedding scheme work in the presence of wind.

Bus	Type	V (p.u.)	Angele (degrees)	PG (MW)	QG (MVAR)	PL (MW)	QL (MVAR)
1	swing	1.04	0	148.025	6.478	-	-
2	constant voltage	1.039	-9.45	0	0	-	-
3	constant voltage	1.025	-2.998	85	-24.54	-	-
4	Load	1.039	-4.523	-	-	-	-
5	Load	1.017	-8.998	-	-	96	50
6	Load	1.038	-6.957	-	-	62	17
7	Load	1.039	-9.45	-	-	-	-
8	Load	1.031	-9.49	-	-	73	27
9	Load	1.04	-5.67	-	-	-	-
Total				233.025	-18.062	231	94
Percentage shed						26.67%	18.26%

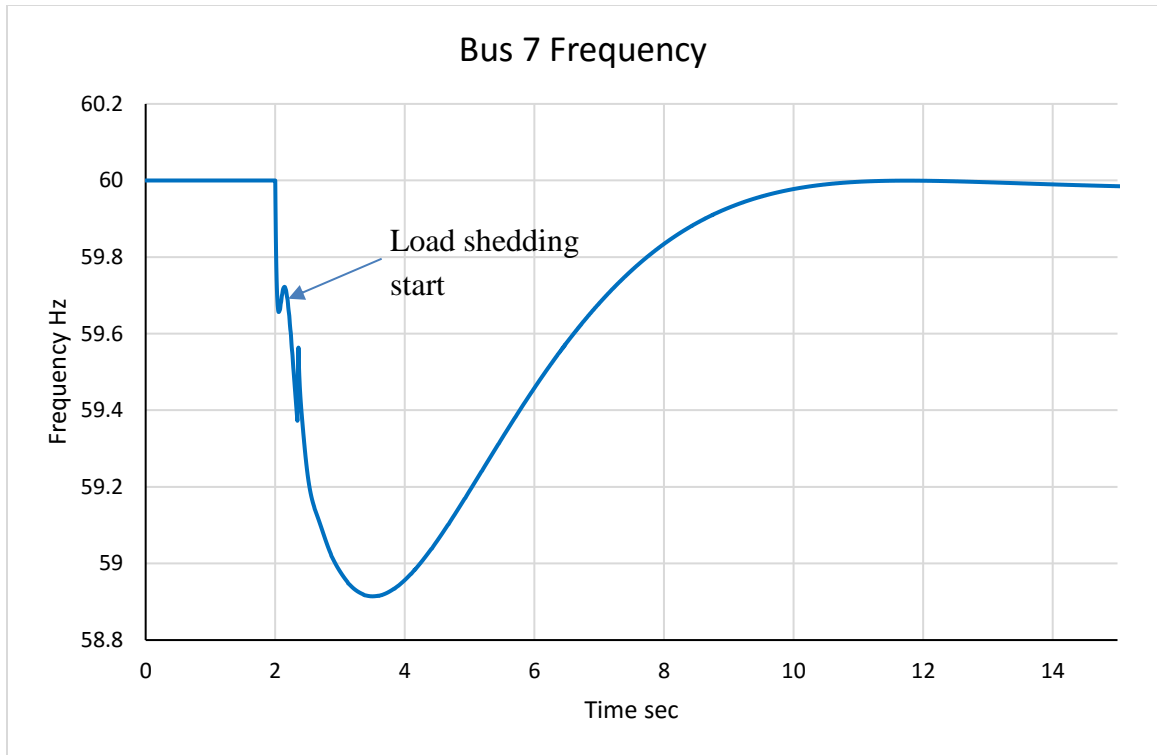


**Figure 4.18. Bus 7 frequency response after load shedding**

The frequency drops to 58.9 Hz (Figure 4.18) after load shedding is triggered and dropped the calculated load to be shed (Table 4.6). The frequency is restored to the nominal operation level after 8 seconds from starting load shedding as shown in Figure 4.18.

The voltage at the load bus and all system buses should be within the limit. Figure 4.19 shows that all voltages at load buses are within limit

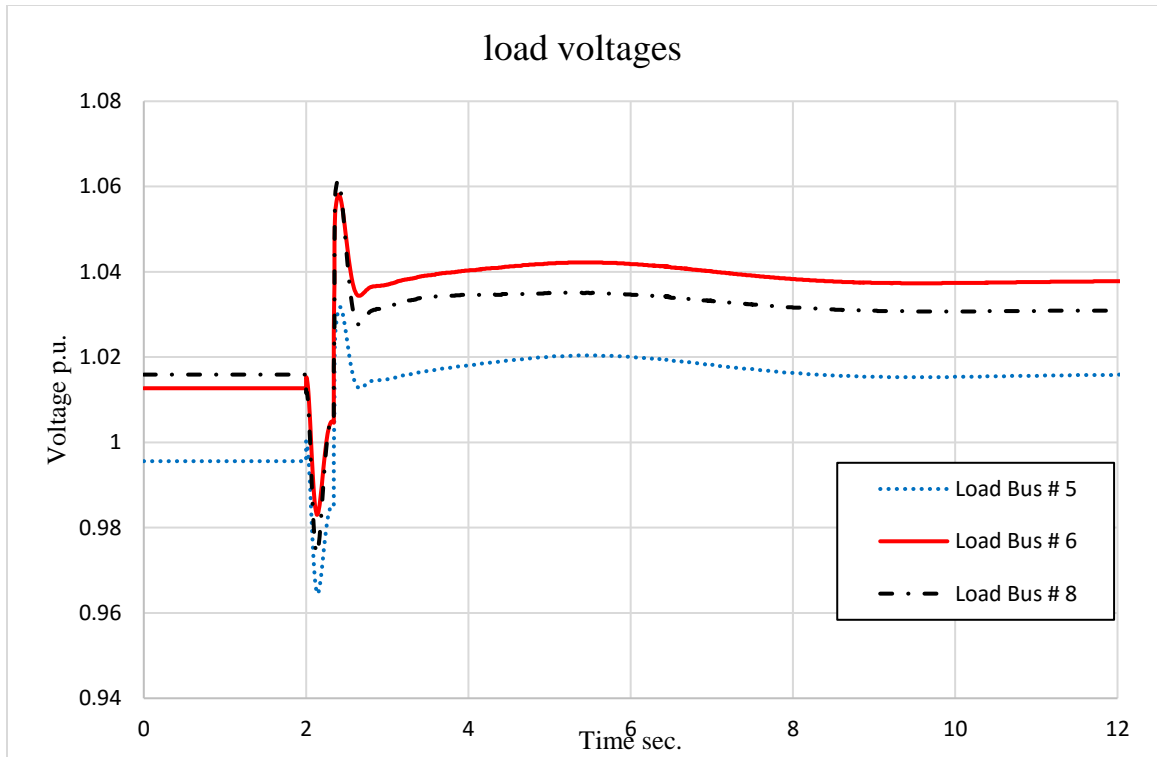


Figure 4.19. Load voltages after load shedding

### 4.3 Study system 2: New England 39 bus system

To verify the validity of the proposed scheme, it will be tested on New England 39 bus system. The tests mostly similar to what is performed on 9 bus system. Figure 4.20 shows the single line diagram for the test system in Powerworld simulator platform.

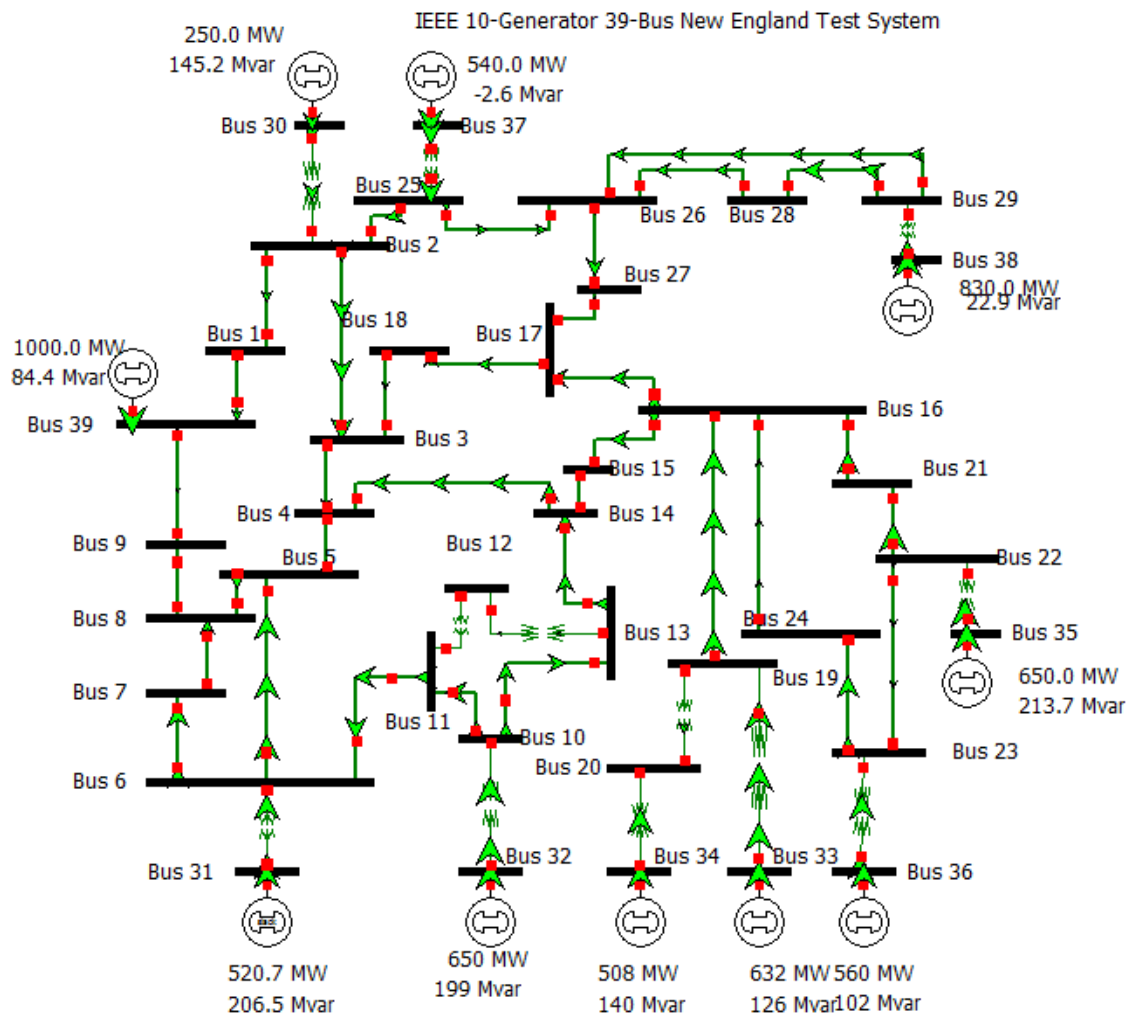
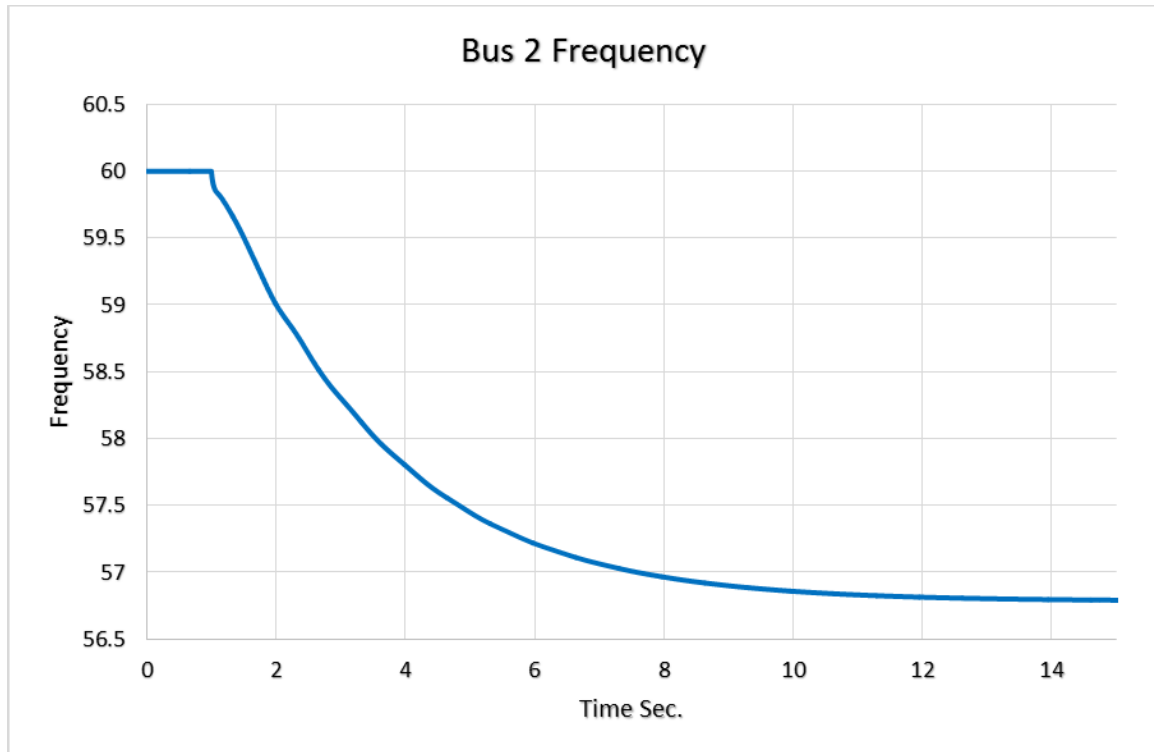


Figure 4.20. New England 39 bus system

Figure 4.21 show the frequency response at bus 2 following the loss of generator 9. The frequency starts to decline after the loss of generator 9 at bus 38 with initial loading of 830 MW. The frequency settles at around 57 Hz, which is not acceptable operation situation and a correction action needs to be carried out.

For this system, the voltage deviation limit increased to be  $\pm 0.1$  p.u.



**Figure 4.21 Frequency at bus 2 following major disturbance without load shedding**

In the following sections, load shedding schemes will be applied to alleviate the frequency drop problem. The proposed load shedding and conventional load shedding are the schemes that will be used.

### 4.3.1 Conventional load shedding

Here the conventional load shedding results are examined and presented. The total load shed by the scheme is 10%.

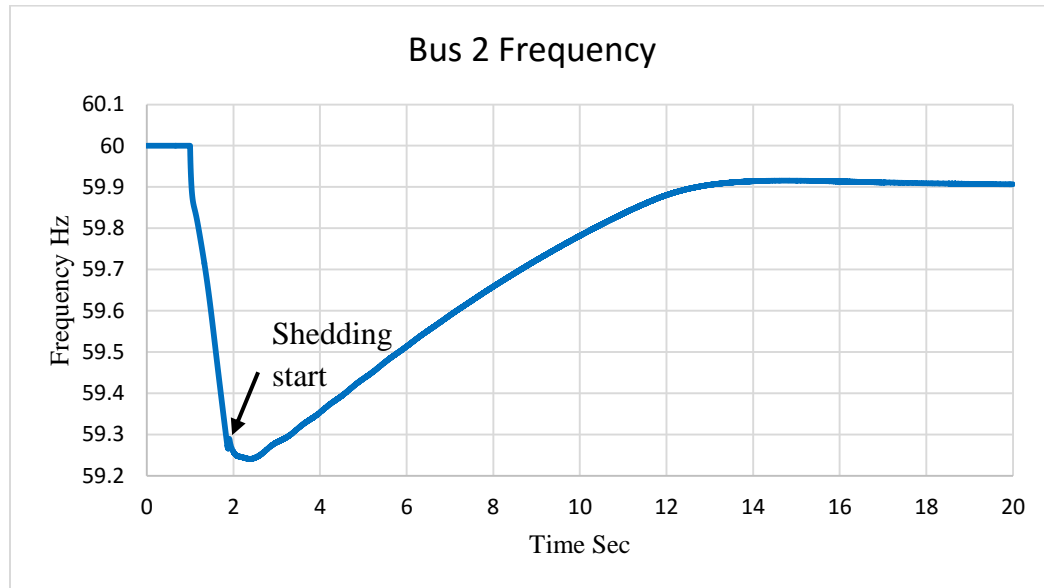
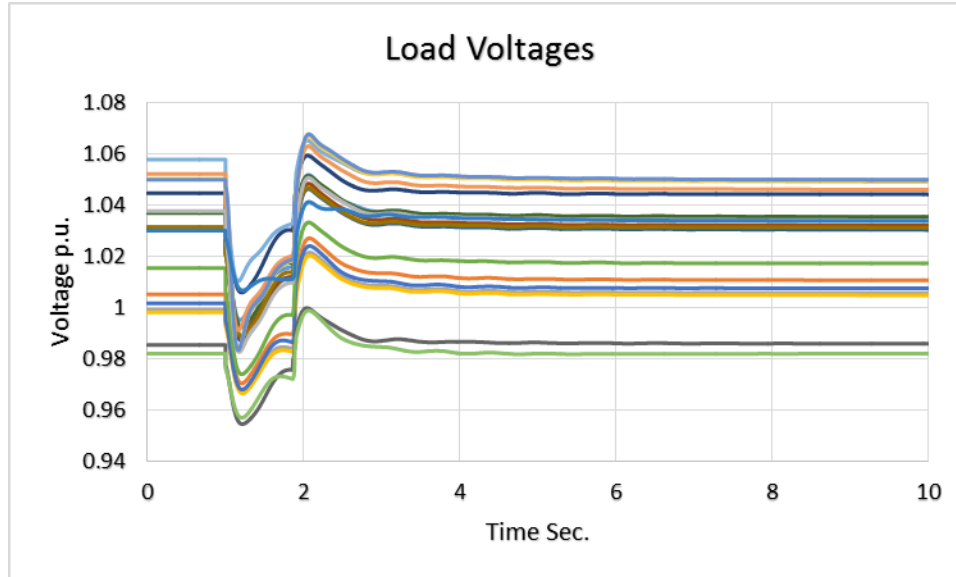


Figure 4.22. Frequency response after conventional load shedding

Figure 4.22 shows that the frequency drops to 59.25 Hz after load shedding is initiated and stabilize at 59.9 Hz after 10 seconds. According to the design of conventional load shedding scheme Table 4.1, the amount of load shed is not enough to bring the balance between the generation and load. This is one of the drawbacks of the conventional load shedding scheme. The bus voltages due to conventional load shedding are shown in Figure 4.23.



**Figure 4.23. Load voltage after conventional load shedding**

All the voltages are within the limit because the reactive power supplied by the lost machine is not high and the amount of curtailed reactive power is less (10%) (Figure 4.23).

### **4.3.2 Optimal load shedding**

The bus data output for 39 bus system at healthy conditions and after the optimal load shedding is carried out is given in the Appendix B. Table 4.7 shows the percentage load shed from each load bus due to loss of generator 9 with initial loading of 830 MW. The results show that the program selects specified candidate buses for the load shedding process. For example, the amount of load shed from bus 15 is 20% while no load shed from buses 3, 4, and 7.

**Table 4.7 Percentage load shedding after loss generator 9 in IEEE 39 bus system**

<b>Load Buses</b>	<b>Time Delay</b>	<b>Breaker Time</b>	<b>% MW Shed</b>	<b>% MVAR Shed</b>
<b>bus 3</b>	0.1	0.1	0%	0%
<b>bus 4</b>	0.1	0.1	0%	0%
<b>bus 7</b>	0.1	0.1	0%	0%
<b>bus 8</b>	0.1	0.1	0%	15%
<b>bus 12</b>	0.1	0.1	0%	0%
<b>bus 15</b>	0.1	0.1	20%	0%
<b>bus 16</b>	0.1	0.1	0%	0%
<b>bus 18</b>	0.1	0.1	4%	17%
<b>bus 20</b>	0.1	0.1	20%	25%
<b>bus 21</b>	0.1	0.1	20%	25%
<b>bus 23</b>	0.1	0.1	13%	25%
<b>bus 24</b>	0.1	0.1	7%	25%
<b>bus 25</b>	0.1	0.1	10%	15%
<b>bus 26</b>	0.1	0.1	0%	0%
<b>bus 27</b>	0.1	0.1	20%	8%
<b>bus 28</b>	0.1	0.1	11%	25%
<b>bus 29</b>	0.1	0.1	17%	0%
<b>bus 31</b>	0.1	0.1	0%	0%
<b>bus 39</b>	0.1	0.1	20%	0%
		<b>Total</b>	<b>11%</b>	<b>7%</b>

Applying the results presented in Table 4.7 on the test system implemented in Powerworld simulator the response of the frequency is demonstrated in Figure 4.24.



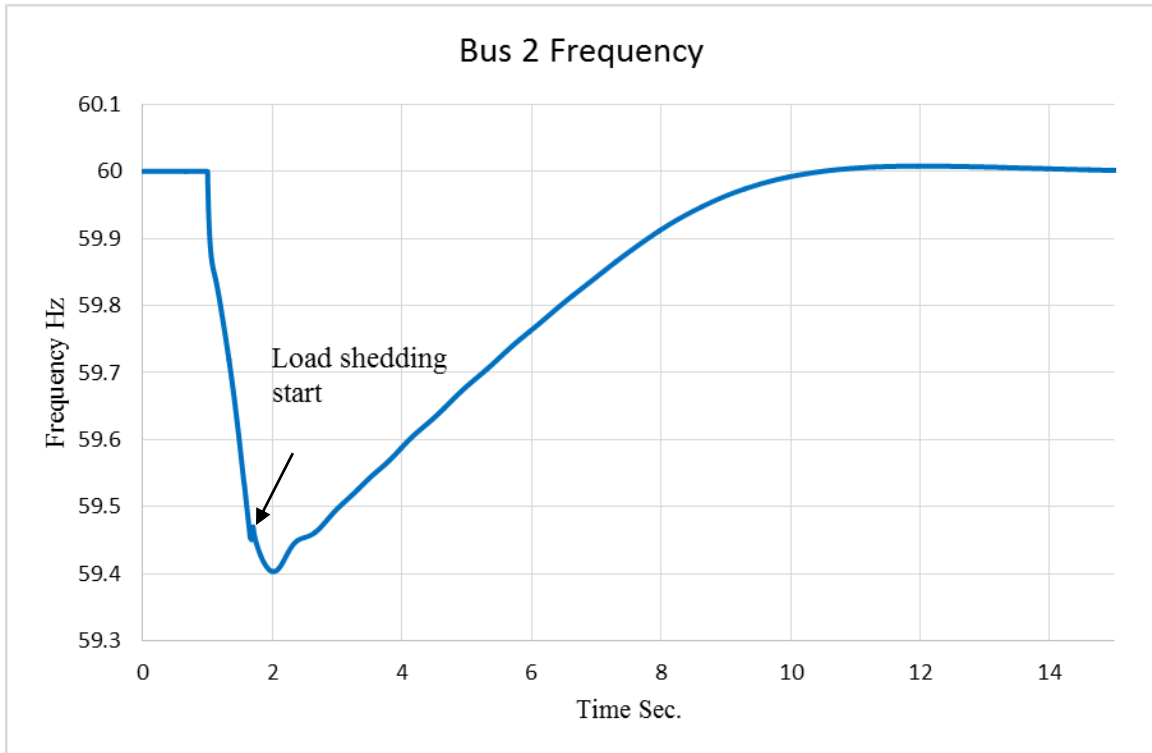


**Figure 4.24 Frequency response after optimal load shedding.**

Because of the delay associated with pickup frequency and breaker delay time the load shedding start at 59.45 Hz (the pickup frequency is adjusted to 59.6 Hz). Figure 4.24 shows that the frequency drops to 59.4 after load shedding is initiated and stabilizes at the nominal value after 8 seconds from starting load shedding.

Figure 4.25 shows the voltage at load buses. All the values are within the specified limit.

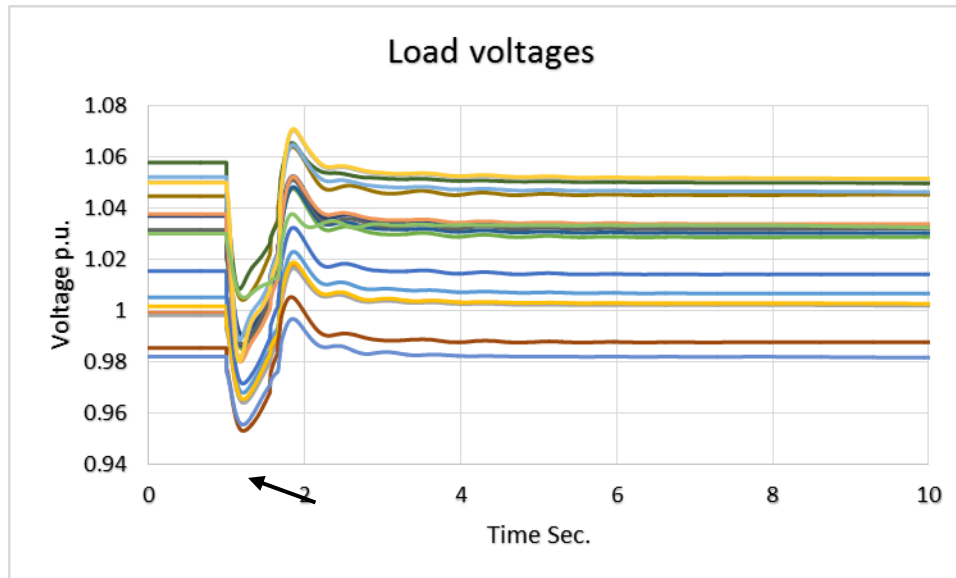


Figure 4.25. Load voltages after load shedding

Figure 4.26 compares between the optimal load shedding and conventional load shedding schemes. The total MW curtailed is 11 % and total MVAR is 7 % from the optimal scheme. This value brings back the frequency to operation level and preserves the load voltage within limits.

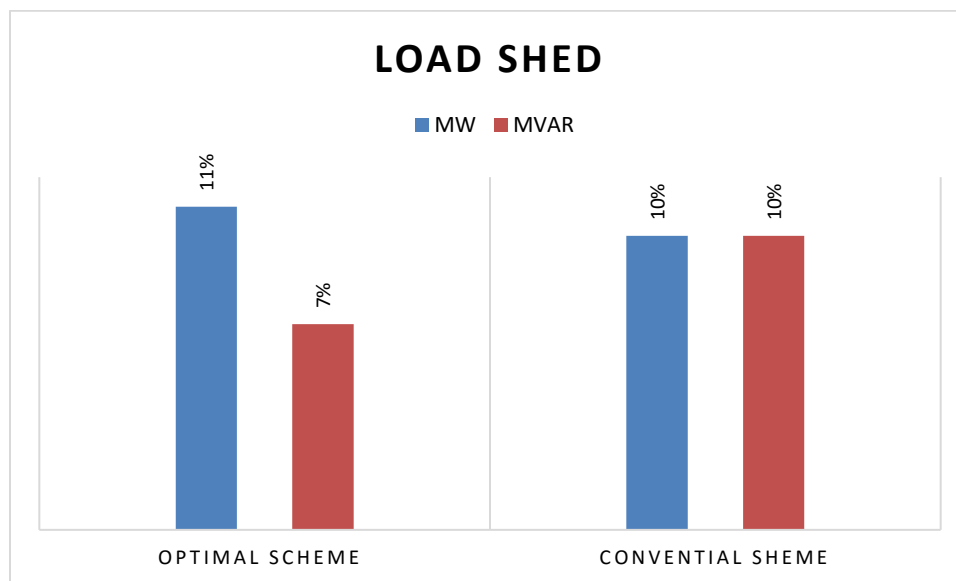


Figure 4.26. Load shed comparison

Although the conventional load shedding scheme according to the design in Table 4.1 shed less MW than optimal scheme but this amount of load shed is not sufficient to restore the frequency to the nominal value as shown in Figure 4.22. As mentioned in the previous discussion, the conventional load shedding scheme deals with the load represented as apparent power (MVA), so that, usually the amount of reactive and active power shed from the load is equal. Whereas the proposed optimal load shedding deals with reactive and active power separately Figure 4.26.

### 4.3.3 Case 5 loss transmission lines 5-8 and 7-8

To show and demonstrate the functionality of the proposed scheme in case of under voltage, two contingency events were carried by taking lines 5-8 and 7-8 out of service. Due to this action, the bus voltage drops at two buses below 0.9 p.u. as shown in Figure 4.27. The frequency of the system is affected by this disturbance. The frequency stabilizes above 60 Hz with +0.15 Hz deviation as shown in Figure 4.28.

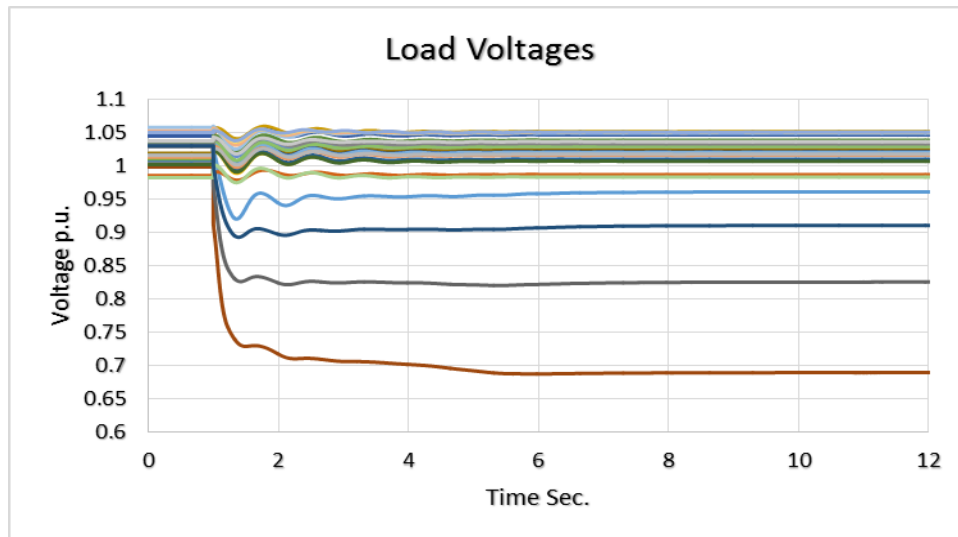
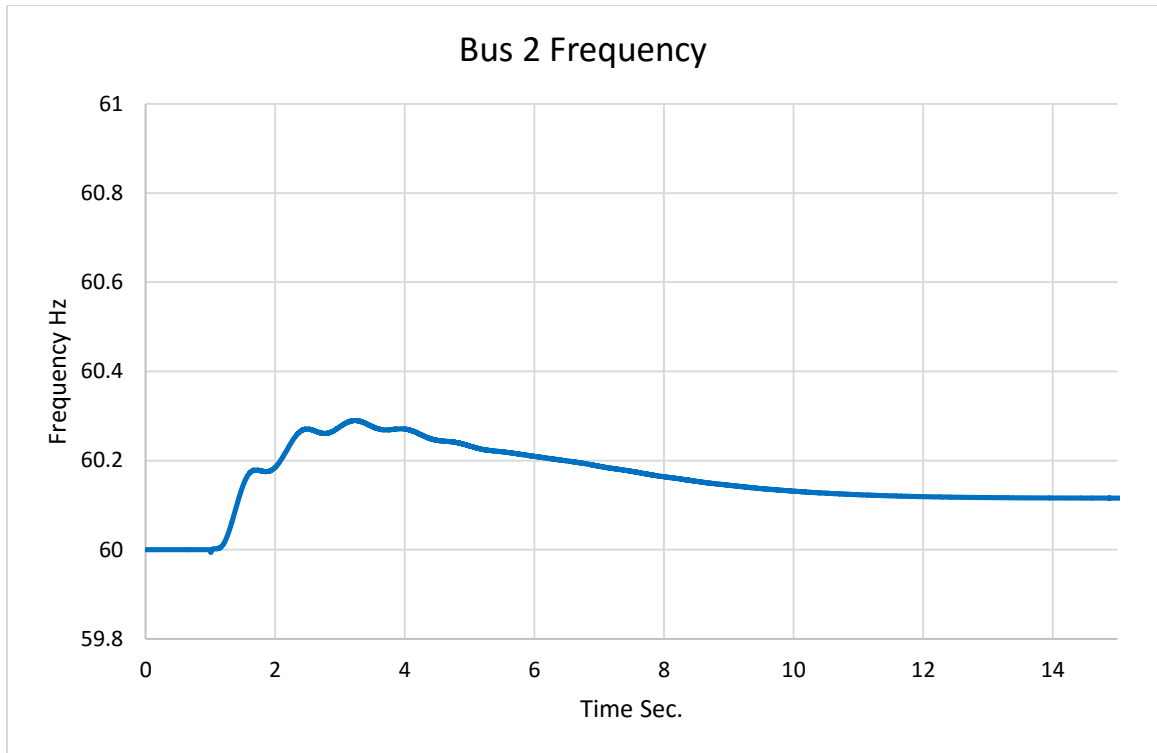


Figure 4.27. Load voltage due to lines loss



**Figure 4.28. Frequency response due to lines loss**

To eliminate the under voltage in the system, the optimal load shedding scheme suggests shedding a reactive power from the affected buses. The values presented in Table 4.8 indicate there is no need to shed active power. Shedding of reactive power can be expressed as switching on shunt capacitors coordinated with load shedding relays.

**Table 4.8. Load shed results**

<b>Load Buses</b>	<b>Time Delay Sec.</b>	<b>Breaker Time Sec</b>	<b>% MW Shed</b>	<b>% MVAR Shed</b>
<b>bus 7</b>	0.1	0.1	0	100%
<b>bus 8</b>	0.1	0.1	0	100%

Applying the above setting to the system, the voltage profile for the system will be within the limit as shown in Figure 4.29.

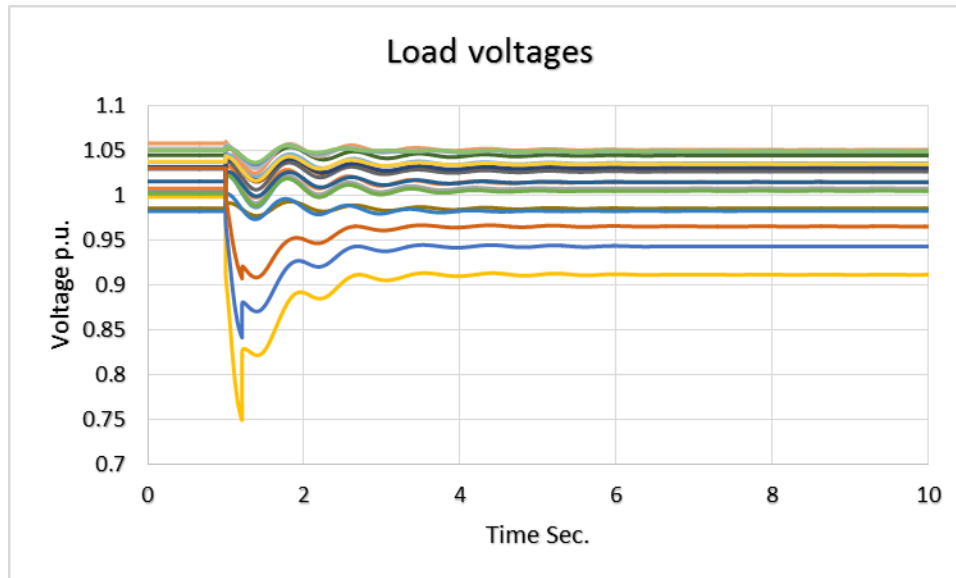


**Figure 4.29. Load voltage after load shedding**

Figure 4.29 shows that the voltage drop problem is remedied by the optimal load shedding scheme.

The frequency of the system, after load shedding, should be within the limit to insure that the load shedding due to voltage drops does not cause frequency instability.

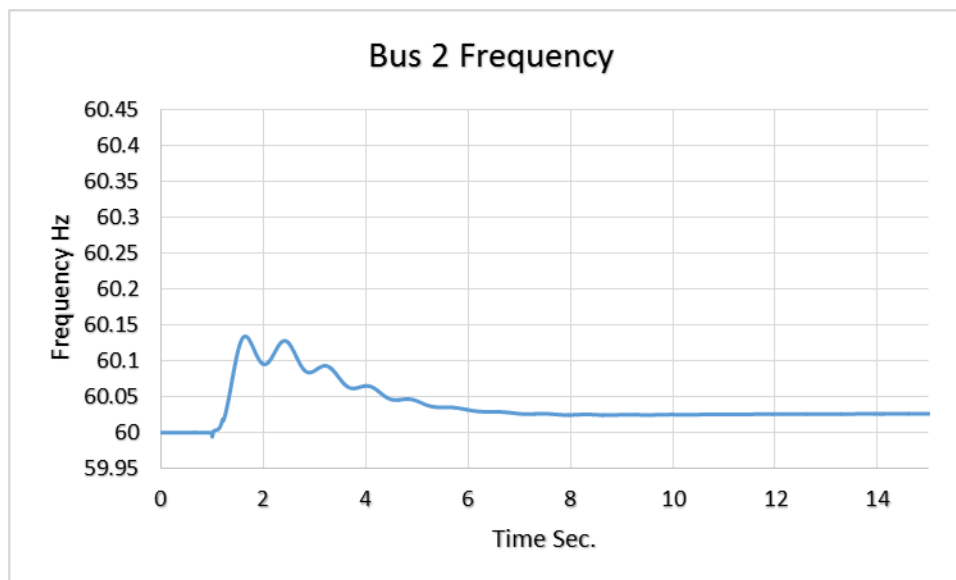


**Figure 4.30. Frequency response after load shedding.**

Figure 4.30 depicts the frequency response after load shedding. It is almost 60 Hz.

#### 4.4 Study system of New England 39 bus system in presence of wind turbine

As in the case of 9 bus system, the presence of wind power plant in the power system will be studied for load shedding. Generator 3 with initial loading 650 MW is considered as a wind power plants.

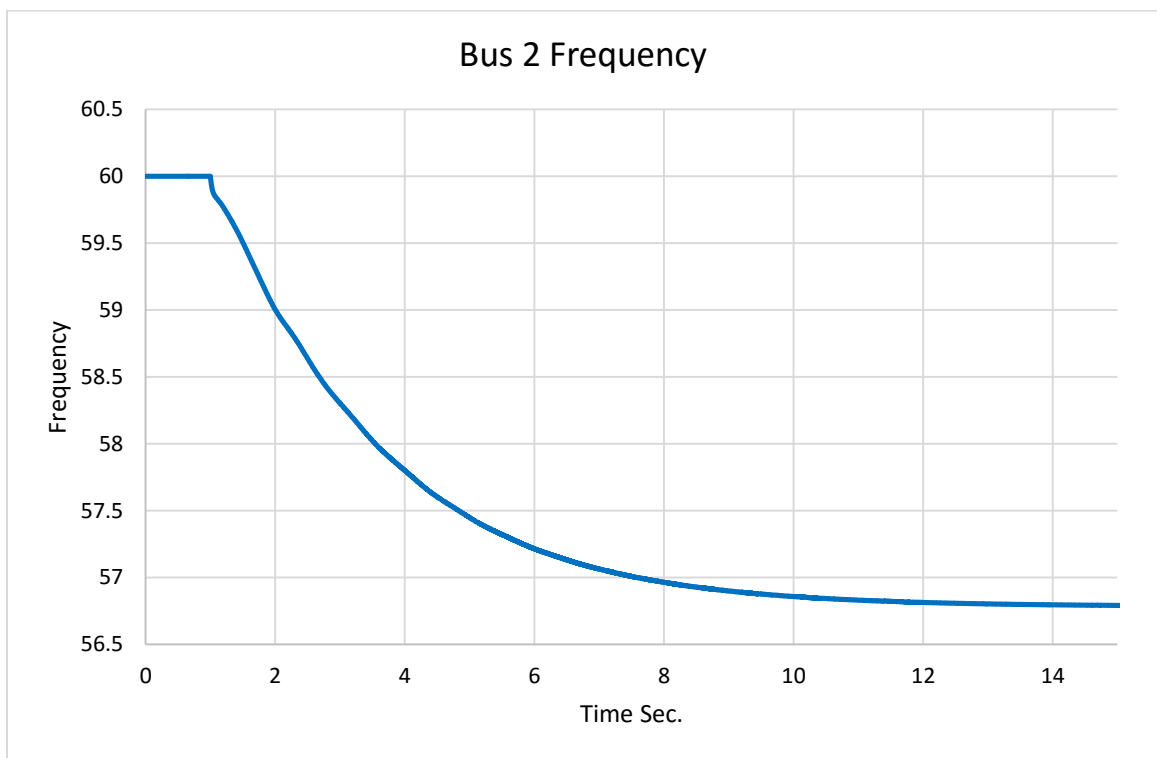


Figure 4.31. Frequency response during major disturbance in presence of wind

Figure 4.31 shows the frequency response of the system in the presence of wind turbine. The frequency drops to 56.8 Hz in 14 seconds. This value is lower than the frequency response presented in (Figure 4.21) without the existence of wind turbine in the system.

The load shedding carried out to correct this situation will be presented in the subsequent sections.

#### 4.4.1 Conventional load shedding results

In this section, the results due to conventional load shedding will be presented. The scheme will shed 10% from active and reactive power.

Figure 4.32 shows the frequency response after load shedding. The frequency drops to 59.2 Hz after the load shedding is engaged and dropped the specified amount of load to be shed. After 12 seconds from load shedding starting, the frequency settled at 59.9 Hz (Figure 4.32). Figure 4.33 shows the load voltage after load shedding and there is no violation according to the criteria for the voltage limit in this system.

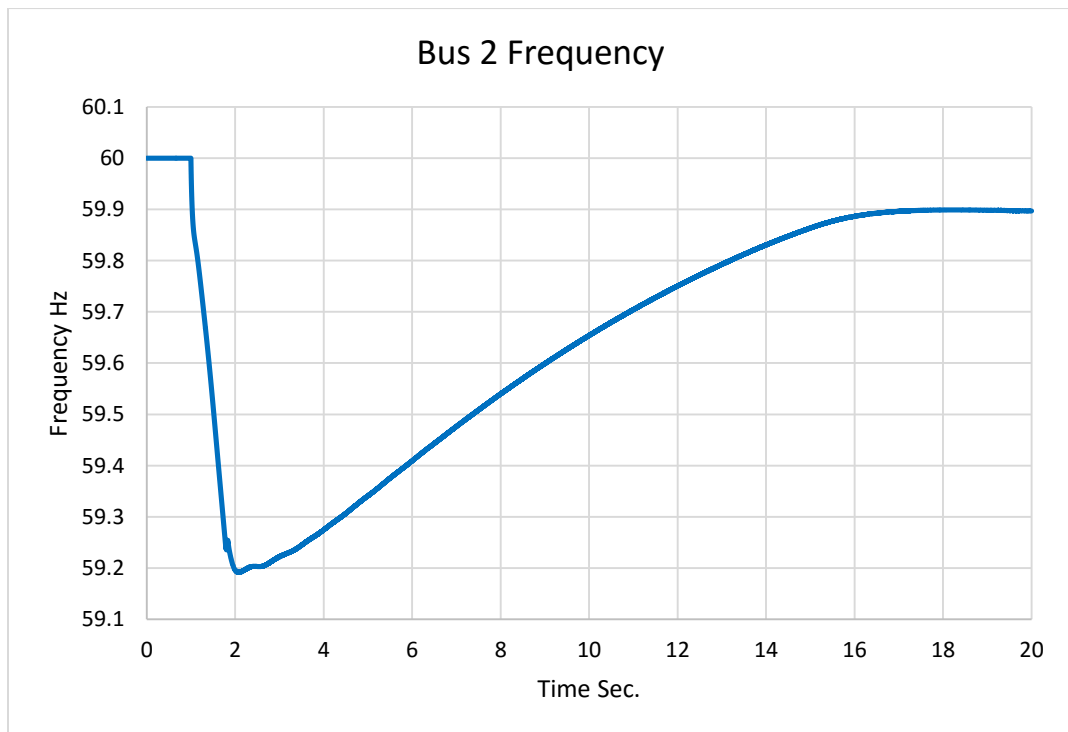


Figure 4.32. Frequency response after load shedding

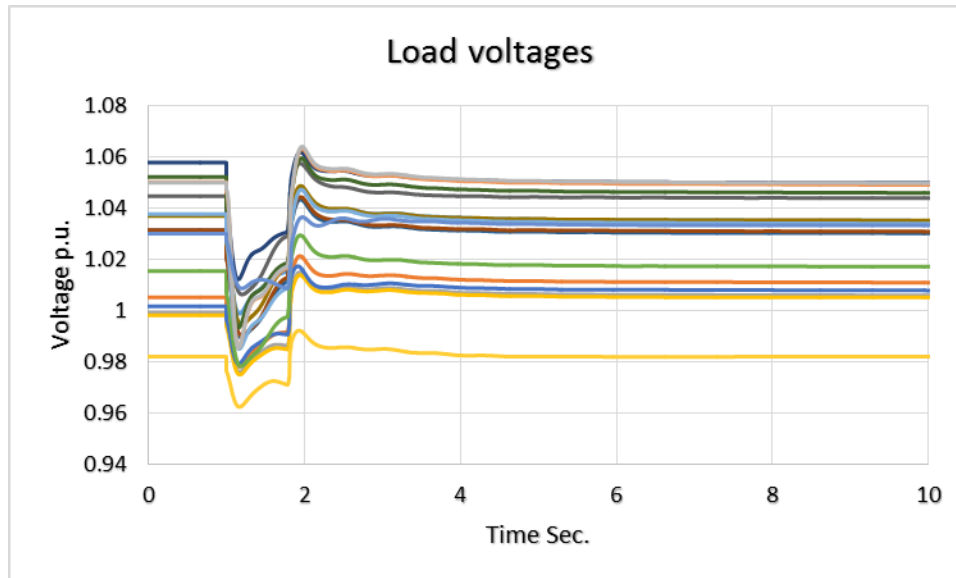


Figure 4.33. Load voltage after load shedding

#### 4.4.2 Optimal load shedding results

The bus data output for the system after load shedding in the presence of Wind turbine is given in Appendix B.

Table 4.9 shows the results from optimal load shedding in the presence of wind turbine. The scheme sheds according to the effect of the load on voltages. For instance, in bus 7 and 8 there is 0% active power shed and 25 % reactive power shed whereas in bus 15 there is 20 % active power shed and 0 % reactive power shed.

The total load shed in this event is more than the load shed the case when there is no wind turbine in the system as shown Table 4.9.



Table 4.9. Load shedding results

Load Buses	Time Delay Sec.	Breaker Time Sec.	% MW Shed	% MVAR Shed
bus 3	0.1	0.1	0%	0%
bus 4	0.1	0.1	0%	0%
bus 7	0.1	0.1	0%	25%
bus 8	0.1	0.1	0%	25%
bus 12	0.1	0.1	0%	25%
bus 15	0.1	0.1	20%	0%
bus 16	0.1	0.1	0%	9%
bus 18	0.1	0.1	11%	23%
bus 20	0.1	0.1	20%	9%
bus 21	0.1	0.1	13%	19%
bus 23	0.1	0.1	20%	0%
bus 24	0.1	0.1	16%	0%
bus 25	0.1	0.1	20%	13%
bus 26	0.1	0.1	20%	24%
bus 27	0.1	0.1	20%	25%
bus 28	0.1	0.1	8%	22%
bus 29	0.1	0.1	12%	26%
bus 31	0.1	0.1	0%	0%
bus 39	0.1	0.1	20%	25%
Total			12%	17%

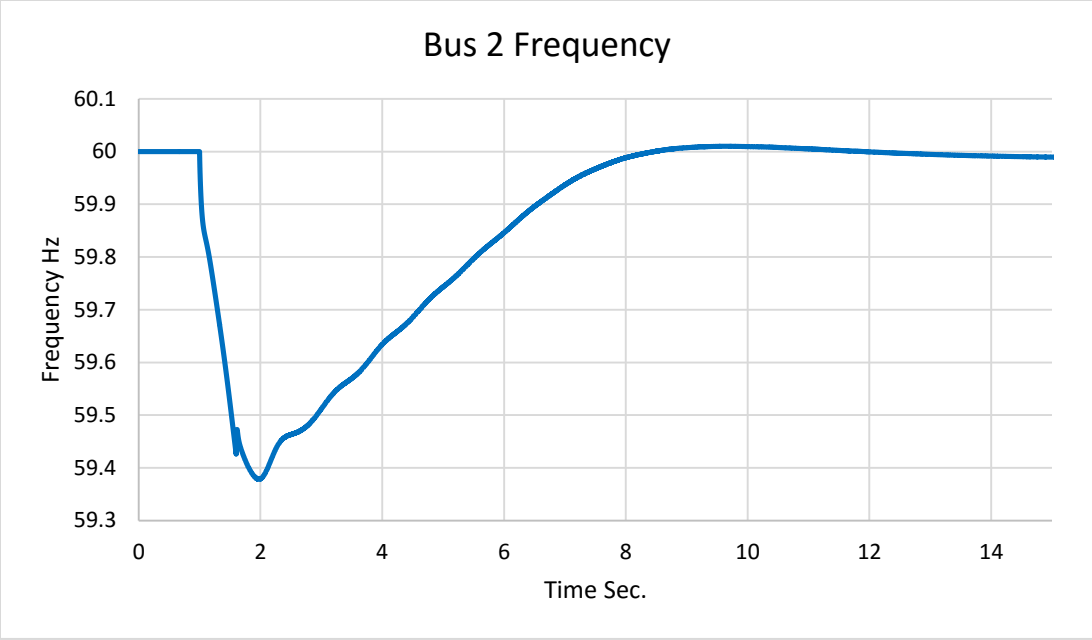


**Figure 4.34. Frequency response after load shedding**

Frequency response is depicted in Figure 4.34. The frequency drops to 59.38 Hz after load shedding initiated and rising in 6 seconds to 60 Hz and settled at that level.

Voltage after load shedding is shown in Figure 4.35. All values are within acceptable limits.

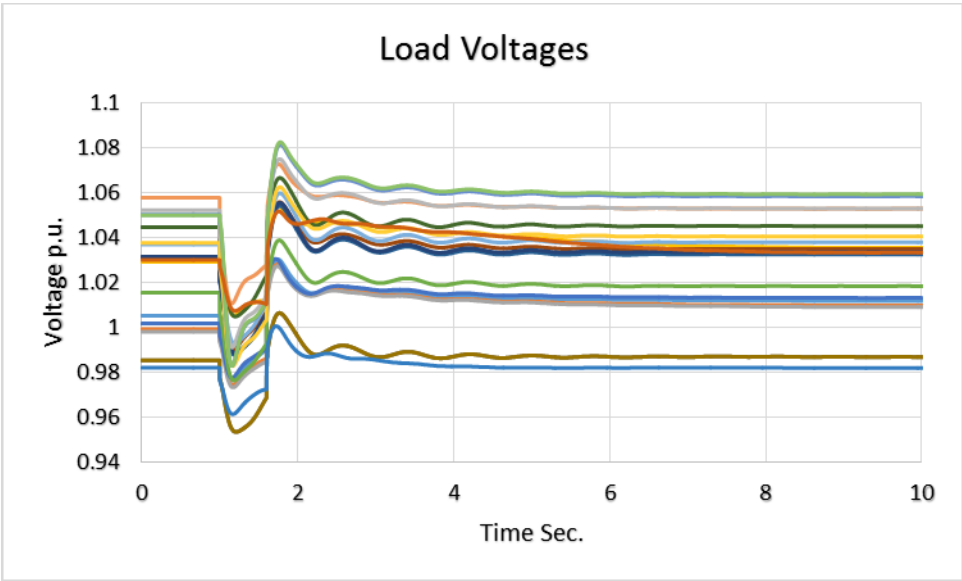


**Figure 4.35. Load voltage after load shedding**

## **CHAPTER 5**

### **CONCLUSION**

#### **5.1 Conclusion**

The objective of this study is to develop optimal load shedding scheme that responds to the frequency and voltage reduction. The algorithm uses load flow technique to decide the optimal load to be shed and the appropriate locations for load shedding to take place. In the case of frequency based events the algorithm considers the voltage stability issue after load shedding to be within specified limits (constraints). The load shedding due to voltage events considers the frequency stability issue satisfying system constraints. The WECC 9 bus system and New England 39 bus system tests are used to test the scheme.

Particle Swarm Optimization (PSO) algorithm is used to solve the constrained objective function implemented in MATLAB. The output of the algorithm is applied to Powerworld simulator for transient analysis purpose. The results show that the optimal scheme is able to restore the frequency to the operation level in case of under-frequency events. It is able to secure the voltage within the acceptable and secure values in the case of under voltage event.

Wind power plant is implemented in the generation of test systems to show the effect of the presence of the renewable resources on load shedding. The optimal load shedding scheme gives good results in the presence of the wind with a little increase in the amount

of the load to be shed because wind power plants do not inherently have an inertial response, generators are effectively isolated from the grid by the converter dynamics.

The optimal load shedding scheme is compared to a published work. The proposed scheme shed about 50% less load than the compared work. The advantage of the proposed scheme is simplicity in structure and effectiveness in distributing the load to be shed among load buses.

## **5.2 Future works**

- The scheme can be tested in real time based software to pave the way of using it in industrial application
- A programmed protection device can be added to shed or sent a trip signal based on optimal load shedding scheme calculation.
- Study the existence of renewable resources on a long term scale and their effects on the optimal load scheme without disturbance i.e. study the variability nature of these sources.

## References

- [1] P. Kundur, *Power system stability and control*. New York: McGraw-Hill, 1994.
- [2] R. Miller and A. H. Robbins, *Circuit Analysis: Theory and Practice*, Fifth Edit. Cengage Learning, 2013.
- [3] J. Zhu, *Optimization of Power System Operation*, 2nd Editio. Wiley-IEEE Press, 2014.
- [4] “What is underfrequency load shedding?,” *Guam Power Authority*, 2015. [Online]. Available: [http://guampowerauthority.com/gpa\\_authority/engineering/gpa\\_engineering\\_under\\_frequency\\_loadshedding.php](http://guampowerauthority.com/gpa_authority/engineering/gpa_engineering_under_frequency_loadshedding.php).
- [5] C. Mozina, “Undervoltage load shedding,” *Electr. Energy T&D Mag.*, pp. 26–32, 2006.
- [6] C. W. Taylor, “Concepts of undervoltage load shedding for voltage stability,” *IEEE Trans. Power Deliv.*, vol. 7, no. 2, pp. 480–488, 1992.
- [7] L. Zhang and J. Zhong, “UFLS design by using  $f$  and integrating  $df/dt$ ,” *2006 IEEE PES Power Syst. Conf. Expo. PSCE 2006 - Proc.*, no. c, pp. 1840–1844, 2006.
- [8] J. J. Ford, H. Bevrani, and G. Ledwich, “Adaptive load shedding and regional protection,” *Int. J. Electr. Power Energy Syst.*, vol. 31, no. 10, pp. 611–618, 2009.
- [9] F. Shokooh, J. J. Dai, S. Shokooh, J. Taster, H. Castro, T. Khandelwal, and G. Donner, “Intelligent Load Shedding Need for a Fast and Optimal Solution,” *Ind. Appl. Conf. 2005. Fourtieth IAS Annu. Meet. Conf. Rec. 2005*, vol. 1, pp. 417–425, 2005.
- [10] P. M. Joshi, “Load shedding algorithm using voltage and frequency data,” *Masters Abstr. Int.*, no. December, p. 96, 2007.
- [11] J. Tang, J. Liu, F. Ponci, and a Monti, “Adaptive load shedding based on combined frequency and voltage stability assessment using synchrophasor measurements,” *Power Syst. IEEE Trans.*, vol. 28, no. 2, pp. 2035–2047, 2013.
- [12] A. A. M. Zin, H. M. Hafiz, and W. K. Wong, “Static and dynamic under-frequency load shedding: a comparison,” *2004 Int. Conf. Power Syst. Technol. 2004. PowerCon 2004.*, vol. 1, no. November, pp. 941–945, 2004.
- [13] H. Mokhlis, H. Mohamad, A. H. A. Bakar, and M. Karimi, “Under-Frequency Load Shedding scheme for islanded distribution network connected with mini hydro,” *Int. J. Electr. Power Energy Syst.*, vol. 42, no. 1, pp. 127–138, 2012.

- [14] S. Abdelwahid, A. Babiker, A. Eltom, and G. Kobet, "Hardware Implementation of an Automatic Adaptive Centralized Underfrequency Load Shedding Scheme," *IEEE Trans. POWER Deliv.*, vol. 29, no. 6, pp. 2664–2673, 2014.
- [15] N. Xia, H. B. Gooi, A. Abur, S. X. Chen, Y. S. F. Eddy, and W. Hu, "Enhanced state estimator incorporating adaptive underfrequency load shedding under contingencies via the alternating optimization method," *Int. J. Electr. Power Energy Syst.*, vol. 81, pp. 239–247, 2016.
- [16] X. Wu, P. Jiang, and J. Lu, "Multiagent-based distributed load shedding for islanded microgrids," *Energies*, vol. 7, no. 9, pp. 6050–6062, 2014.
- [17] K. . A. Palaniswamy and J. Sharma, "Optimum load shedding taking into account of voltage and frequency characteristics of loads," *IEEE Trans. Power Appar. Syst.*, vol. PAS-104, no. 6, pp. 689–692, 1985.
- [18] Adel A. Abou-El-Ela, A. Z. El-Din, and S. R. Spea, "Optimal load shedding in power systems," *2006 Elev. Int. Middle East Power Syst. Conf.*, vol. 2, pp. 568–575, 2006.
- [19] H. Çimen and M. Aydın, "Optimal Load Shedding Strategy for Selçuk University Power System with Distributed Generation," *Procedia - Soc. Behav. Sci.*, vol. 195, pp. 2376–2381, 2015.
- [20] R. Mageshvaran and T. Jayabarathi, "Steady state load shedding to mitigate blackout in power systems using an improved harmony search algorithm," *Ain Shams Eng. J.*, vol. 6, no. 3, pp. 819–834, 2015.
- [21] Z. Liu, F. Wen, and G. Ledwich, "An optimal under-frequency load shedding strategy considering distributed generators and load static characteristics," *Int. Trans. Electr. ENERGY Syst.*, vol. 24, pp. 79–90, 2014.
- [22] S. Arnborg, G. Andersson, D. J. Hill, and I. A. H. Iskens, "On undervoltage load shedding in power systems," *Electr. Power Energy Syst. Sci. Ltd*, vol. 19, no. 2, pp. 141–149, 1997.
- [23] E.-S. Mz, M. Ga, D. Mm, and R. Wi, "Optimum load shedding for avoiding steady state voltage instability," *Electr. Power Syst. Res.*, vol. 50, no. 2, pp. 199–213, 1999.
- [24] L. D. Arya, P. Singh, and L. S. Titare, "Optimum load shedding based on sensitivity to enhance static voltage stability using de," *Swarm Evol. Comput.*, vol. 6, pp. 25–38, 2012.
- [25] A. Mahari and H. Seyedi, "A wide area synchrophasor-based load shedding scheme to prevent voltage collapse," *Int. J. Electr. Power Energy Syst.*, vol. 78, pp. 248–257, 2016.
- [26] P.M. Anderson and A.A. Fouad, *Power System Control and Stability*, 2nd Editio. Wiley-IEEE Press, 2002.

- [27] “IEEE 39-Bus System,” (*ICSEG*), *Illinois Center for a Smarter Electric Grid*. [Online]. Available: <http://icseg.itl.illinois.edu/ieee-39-bus-system/>. [Accessed: 03-Apr-2016].
- [28] PowerWorld Coroperation, “TransientModels\_PDF.” [Online]. Available: [http://www.powerworld.com/WebHelp/Content/TransientModels\\_PDF/](http://www.powerworld.com/WebHelp/Content/TransientModels_PDF/). [Accessed: 29-Mar-2016].
- [29] T. O. J. Duncan Glover, Mulukutla S. Sarma, *Power System Analysis and Design*, Fifth Edit. Cengage Learning, 2011.
- [30] A.-H. S. Soliman and A.-A. H. Mantawy, *Modern Optimization Techniques with Applications in Electric Power Systems*. 2012.
- [31] M. A. Abido, “Optimal power flow using particle swarm optimization,” *Int. J. Electr. Power Energy Syst.*, vol. 24, no. 7, pp. 563–571, 2002.
- [32] J. Kennedy and R. Eberhart, “Particle swarm optimization,” *Neural Networks, 1995. Proceedings., IEEE Int. Conf.*, vol. 4, pp. 1942–1948 vol.4, 1995.
- [33] H. E. Lokay and V. Burtnyk, “Application of Underfrequency Relays for Automatic Load Shedding,” *IEEE Trans. Power Appar. Syst.* , no. 3, pp. 776–783, 1968.
- [34] D. Xu, “Optimal Load Shedding and Restoration,” *A Diss. Present. to Grad. Sch. Clemson Univ.*, 2001.
- [35] WECC Renewable Energy Modeling Task Force, “WECC Wind Power Plant Dynamic Modeling Guide,” 2010.

# APPENDICES

## APPENDIX A: Test systems data

### Nomenclature

<b>Rated power (MVA)</b>	Machine-rated MVA; base MVA for impedances
<b>Rated voltage (kV)</b>	Machine-rated terminal voltage in kV; base kV for impedances
<b><math>H</math> (s)</b>	Inertia constant in s
<b><math>D</math></b>	Machine load damping coefficient
<b><math>r_a</math> (p.u)</b>	Armature resistance in p.u.
<b><math>x_d</math> (p.u)</b>	Unsaturated d axis synchronous reactance in p.u.
<b><math>x_q</math> (p.u)</b>	Unsaturated q axis synchronous reactance in p.u.
<b><math>x'_d</math> (p.u)</b>	Unsaturated d axis transient reactance in p.u.
<b><math>x'_q</math> (p.u)</b>	Unsaturated q axis transient reactance in p.u.
<b><math>x''_d</math> (p.u)</b>	Unsaturated d axis sub transient reactance in p.u.
<b><math>x''_q</math> (p.u)</b>	Unsaturated q axis sub transient reactance in p.u.
<b><math>x_l</math> or <math>x_p</math> (p.u)</b>	Leakage or Poitier reactance in p.u.
<b><math>T'_{d0}</math> (s)</b>	d axis transient open circuit time constant in s
<b><math>T'_{q0}</math> (s)</b>	q axis transient open circuit time constant in s
<b><math>T''_{d0}</math> (s)</b>	d axis sub transient open circuit time constant in s
<b><math>T''_{q0}</math> (s)</b>	q axis sub transient open circuit time constant in s
<b>S(1.0)</b>	Machine saturation at 1.0 p.u. voltage in p.u.
<b>S(1.2)</b>	Machine saturation at 1.2 p.u. voltage in p.u.
<b><math>T_r</math> (s)</b>	Regulator input filter time constant in s
<b><math>K_a</math> (p.u)</b>	Regulator gain (continuous acting regulator) in p.u.
<b><math>T_a</math> (s)</b>	Regulator time constant in s
<b><math>V_{Rmax}</math> (p.u)</b>	Maximum regulator output, starting at full load field voltage in p.u.
<b><math>V_{Rmin}</math> (p.u)</b>	Minimum regulator output, starting at full load field voltage in p.u.
<b><math>K_e</math> (p.u)</b>	Exciter self-excitation at full load field voltage in p.u.
<b><math>T_e</math> (s)</b>	Exciter time constant in s
<b><math>K_r</math> (p.u)</b>	Regulator stabilizing circuit gain in p.u.
<b><math>T_r</math> (s)</b>	Regulator stabilizing circuit time constant in s
<b><math>E_1</math></b>	Field voltage value,1 in p.u.
<b><math>SE(E_1)</math></b>	Saturation factor at $E_1$



WECC 9 bus system data taken from [26].

TABLE A.1

LINE DATA FOR WECC 9 BUS SYSTEM						
No of line	From bus	To bus	R	X	B/2	
1	7	8	0.0085	0.07	0.0745	
2	8	9	0.0119	0.1	0.1045	
3	7	5	0.032	0.16	0.153	
4	9	6	0.039	0.17	0.179	
5	5	4	0.01	0.09	0.088	
6	4	6	0.017	0.09	0.079	
7	2	7	0	0.06	0	
8	9	3	0	0.06	1	

TABLE A.2

BUS DATA								
Bus no.	Bus type	V	Pg	Qg	Pl	Ql	Qmin	Qmax
1	1	1.04	-	0	0	0	0	0
2	2	1.025	163	0	0	0	-100	130
3	2	1.025	85	0	0	0	-70	50
4	0	1	0	0	0	0	0	0
5	0	1	0	0	125	50	0	0
6	0	1	0	0	90	30	0	0
7	0	1	0	0	0	0	0	0
8	0	1	0	0	100	35	0	0
9	0	1	0	0	0	0	0	0

\*Bus type 1 slack, 2= PV, 0=PQ.

TABLE A.3

MACHINE AND EXCITER PARATMETERS				
<i>Parameter</i>	Machine 1	Machine 2	Machine 3	Unit
<i>Rated MVA</i>	247.5	192	128	MVA
<i>Kv</i>	16.5	18	13.8	Kv
<i>Power factor</i>	1	0.85	0.85	-
<i>Speed</i>	180	3600	3600	r/min
<i>Xd</i>	0.146	0.8958	1.3125	p.u.
<i>X'd</i>	0.0608	0.1198	0.1813	p.u.
<i>Xq</i>	0.0969	0.8645	1.2578	p.u.
<i>X'q</i>	0.0969	0.1969	0.25	p.u.
<i>Xl</i>	0.0336	0.0521	0.0742	p.u.
<i>T'd0</i>	8.96	6	5.89	sec
<i>T'q0</i>	0	0.535	0.6	sec

<i>H</i>	23.64	6.4	3.01	sec
<i>Ka</i>	20	20	20	-
<i>Ta</i>	0.2	0.2	0.2	sec
<i>Ke</i>	1	1	1	-
<i>Te</i>	0.314	0.314	0.314	sec
<i>Kf</i>	0.063	0.063	0.063	-
<i>Tf</i>	0.35	0.35	0.35	sec

New England 39 bus system taken from [27].

TABLE A.4  
LINE DATA FOR 10 UNIT SYSTEM

No lines	Line Data			Resistance	Reactance	Susceptance	Transformer Tap	
	From bus	to Bus	Magnitude				Angle	
1	1	2	0.0035	0.0411	0.6987	1	0	
2	1	39	0.001	0.025	0.75	1	0	
3	2	3	0.0013	0.0151	0.2572	1	0	
4	2	25	0.007	0.0086	0.146	1	0	
5	3	4	0.0013	0.0213	0.2214	1	0	
6	3	18	0.0011	0.0133	.2138	1	0	
7	4	5	0.0008	0.0128	0.1342	1	0	
8	4	14	0.0008	0.0129	0.1382	1	0	
9	5	6	0.0002	0.0026	0.0434	1	0	
10	5	8	0.0008	0.0112	0.1476	1	0	
11	6	7	0.0006	0.0092	0.113	1	0	
12	6	11	0.0007	0.0082	0.1389	1	0	
13	7	8	0.0004	0.0046	0.078	1	0	
14	8	9	0.0023	0.0363	0.3804	1	0	
15	9	39	0.001	0.025	1.2	1	0	
16	10	11	0.0004	0.0043	0.0729	1	0	
17	10	13	0.0004	0.0043	0.0729	1	0	
18	13	14	0.0009	0.0101	0.1723	1	0	
19	14	15	0.0018	0.0217	0.366	1	0	
20	15	16	0.0009	0.0094	0.171	1	0	
21	16	17	0.0007	0.0089	0.1342	1	0	
22	16	19	0.0016	0.0195	0.304	1	0	
23	16	21	0.0008	0.0135	0.2548	1	0	
24	16	24	0.0003	0.0059	0.068	1	0	
25	17	18	0.0007	0.0082	0.1319	1	0	
26	17	27	0.0013	0.0173	0.3216	1	0	
27	21	22	0.0008	0.014	0.2565	1	0	

28	22	23	0.0006	0.0096	0.1846	1	0
29	23	24	0.0022	0.035	0.361	1	0
30	25	26	0.0032	0.0323	.5130	1	0
31	26	27	0.0014	0.0147	0.2396	1	0
32	26	28	0.0043	0.0474	0.7802	1	0
33	26	29	0.0057	0.0625	1.0290	1	0
34	28	29	0.0014	0.0151	0.249	1	0
35	12	11	0.0016	0.0435	0	1.006	0
36	12	13	0.0016	0.0435	0	1.006	0
37	6	31	0	0.025	0	1.070	0
38	10	32	0	0.02	0	1.070	0
39	19	33	0.0007	0.0142	0	1.07	0
40	20	34	0.0009	0.018	0	1.009	0
41	22	35	0	0.0143	0	1.025	0
42	23	36	0.0005	0.0272	0	1	0
43	25	37	0.0006	0.0232	0	1.025	0
44	2	30	0	0.0181	0	1.025	0
45	29	38	0.0008	0.0156	0	1.025	0
46	19	20	0.0007	0.0138	0	1.06	0

TABLE A. 5  
BUS DATA

Bus	Type	Volts	Load MW	Load MVAR	Gen Load	Gen MVAR
1	0	-	0	0	0	0
2	0	-	0	0	0	0
3	0	-	322	2.4	0	0
4	0	-	500	184	0	0
5	0	-	0	0	0	0
6	0	-	0	0	0	0
7	0	-	233.8	84	0	0
8	0	-	522	176	0	0
9	0	-	0	0	0	0
10	0	-	0	0	0	0
11	0	-	0	0	0	0
12	0	-	7.5	88	0	0
13	0	-	0	0	0	0
14	0	-	0	0	0	0
15	0	-	320	153	0	0
16	0	-	329	32.3	0	0
17	0	-	0	0	0	0

18	0	-	158	30	0	0
19	0	-	0	0	0	0
20	0	-	628	103	0	0
21	0	-	274	115.0	0	0
22	0	-	0	0	0	0
23	0	-	247.5	84.6	0	0
24	0	-	308.6	-92.2	0	0
25	0	-	224	47.2	0	1.0
26	0	-	139	17	0	0
27	0	-	281	75.5	0	0
28	0	-	206	27.6	0	0
29	0	-	283.5	26.9	0	0
30	2	1.0475	0	0	250	-
31	1	0.982	9.2	4.6	0	-
32	2	0.9831	0	0	650	-
33	2	0.9972	0	0	632	-
34	2	1.0123	0	0	508	-
35	2	1.0493	0	0	650	-
36	2	1.0635	0	0	560	-
37	2	1.0278	0	0	540	-
38	2	1.0265	0	0	830	-
39	2	1.03	1104	250	1000	-

\*bus type 1 =slack, 2 PV, 0= PQ.

TABLE A.6  
IEEE 39-Bus TEST SYSTEM MACHINE DATA

Type	GENROU	GENROU	GENROU
Operation	Sync. Gen.	Sync. Gen.	Sync. Gen.

Default Unit no.	30	31, 32, 33	38
		34, 35, 36, 37	39
Rated power (MV A)	590	835	911
Rated voltage (kV)	22	20	26
Rated pf	0.95	0.9	0.9
$H$ (s)	2.3186	2.6419	2.4862
$D$	2.00	2.00	2.00
$ra$ (p.u)	0.0046	0.0019	0.0010
$xd$ (p.u)	2.110	2.183	2.040
$Xq$ (p.u)	2.020	2.157	1.960
$x' d$ (p.u)	0.280	0.413	0.266
$x' q$ (p.u)	0.490	1.285	0.262
$x'' d$ (p.u)	0.215	0.339	0.193
$x'' q$ (p.u)	0.215	0.339	0.193
$x_l$ or $xP$ (p.u)	0.155	0.246	0.154
$T' do$ (s)	4.200	5.690	6.000
$T' qo$ (s)	0.565	1.500	0.900
$T'' do$ (s)	0.032	0.041	0.004
$T'' qo$ (s)	0.062	0.144	0.004
S(1.0)	0.079	0.134	0.340
S(1.2)	0.349	0.617	1.120

TABLE A.7

IEEE 39-Bus TEST SYSTEM EXCITER DATA

Type	IEEE TI	IEEE TI	IEEE TI
Default Unit no.	30	31, 32, 33 34, 35, 36, 37	38
Rated power (MV A)	590	835	911
Rated voltage (kV)	22	20	26
$T_r$ (s)	0.000	0.000	0.000
$K_a$ (p.u)	200	400	50
$T_a$ (s)	0.3575	0.020	0.060
$V_{Rmax}$ (p.u)	5.730	18.300	1.000
$V_{Rmin}$ (p.u)	-5.730	-18.300	-1.00
$K_e$ (p.u)	1.000	1.000	-0.0393
$T_e$ (s)	0.004	0.942	0.440
$K_r$ (p.u)	0.0529	0.030	0.070
$T_r$	1.000	1.000	1.000
E1	4.2975	3.765	3.375
$SE(E_i)$	0.000	0.8147	0.0644

**APPENDIX B:** Bus data output after load shedding

39 bus system

TABLE B.1  
BUS OUTPUT DATA FOR A HEALTHY IEEE 39 BUS SYSTEM

Bus	Type	V (p.u.)	Angele (degrees)	PG (MW)	QG (MW)	PL (MW)	QL (MW)
1	Load	1.047	-8.446	0	0	0	0
2	Load	1.048	-5.758	0	0	0	0
3	Load	1.029	-8.604	0	0	322	2.4
4	Load	1.003	-9.614	0	0	500	184
5	Load	1.005	-8.618	0	0	0	0
6	Load	1.007	-7.955	0	0	0	0
7	Load	0.997	-10.131	0	0	233.8	84
8	Load	0.996	-10.623	0	0	522	176
9	Load	1.028	-10.33	0	0	0	0
10	Load	1.017	-5.43	0	0	0	0
11	Load	1.012	-6.288	0	0	0	0
12	Load	1	-6.247	0	0	7.5	88
13	Load	1.014	-6.101	0	0	0	0
14	Load	1.011	-7.66	0	0	0	0
15	Load	1.014	-7.737	0	0	320	153
16	Load	1.03	-6.182	0	0	329	32.3
17	Load	1.032	-7.302	0	0	0	0
18	Load	1.03	-8.228	0	0	158	30
19	Load	1.045	-0.968	0	0	0	0
20	Load	0.98	-1.956	0	0	628	103
21	Load	1.03	-3.769	0	0	274	115
22	Load	1.049	0.687	0	0	0	0
23	Load	1.044	0.489	0	0	247.5	84.6
24	Load	1.035	-6.062	0	0	308.6	-92.2
25	Load	1.057	-4.367	0	0	224	47.2
26	Load	1.051	-5.529	0	0	139	17
27	Load	1.037	-7.499	0	0	281	75.5
28	Load	1.05	-2.015	0	0	206	27.6
29	Load	1.05	0.746	0	0	283.5	26.9
30	constant voltage	1.048	-3.337	250	148.39	0	0
31	swing	0.982	0	520.91	200.065	9.2	4.6
32	constant voltage	0.983	2.57	650	207.595	0	0
33	constant voltage	0.997	4.261	632	143.362	0	0
34	constant voltage	0.992	3.428	508	116.726	0	0
35	constant voltage	1.049	5.653	650	217.891	0	0

<b>36</b>	constant voltage	1.064	8.347	560	104.282	0	0
<b>37</b>	constant voltage	1.028	2.419	540	2.009	0	0
<b>38</b>	constant voltage	1.027	7.81	830	24.525	0	0
<b>39</b>	constant voltage	1.03	-10.061	1000	89.708	1104	250
Total				6140.91	1254.555	6097.1	1408.9

\*base MVA=100 MVA,  $V_{base}=20\text{Kv}$  for all generator bus and 500Kv for the rest buses

**TABLE B.2**  
**BUS OUTPUT DATA FOR IEEE 39 BUS SYSTEM AFTER LOSS GENERATOR 9**  
**AND LS CONDUCTED**

<b>Bus</b>	<b>Type</b>	<b>V</b> (p.u.)	<b>Angele</b> (degrees)	<b>PG</b> (MW)	<b>QG</b> (MW)	<b>PL</b> (MW)	<b>QL</b> (MW)
<b>1</b>	Load	1.019	-8.503	0	0	0	0
<b>2</b>	Load	1.02	-9.059	0	0	0	0
<b>3</b>	Load	1.002	-11.49	0	0	322	2.4
<b>4</b>	Load	0.977	-11.19	0	0	500	184
<b>5</b>	Load	0.982	-9.525	0	0	0	0
<b>6</b>	Load	0.985	-8.774	0	0	0	0
<b>7</b>	Load	0.974	-10.9	0	0	233.8	84
<b>8</b>	Load	0.973	-11.33	0	0	522	149
<b>9</b>	Load	1.001	-9.449	0	0	0	0
<b>10</b>	Load	0.987	-6.294	0	0	0	0
<b>11</b>	Load	0.985	-7.144	0	0	0	0
<b>12</b>	Load	0.971	-7.167	0	0	7.5	88
<b>13</b>	Load	0.985	-7.078	0	0	0	0
<b>14</b>	Load	0.983	-8.915	0	0	0	0
<b>15</b>	Load	0.988	-9.037	0	0	256	153
<b>16</b>	Load	1.004	-7.767	0	0	329	32.3
<b>17</b>	Load	1.002	-10.63	0	0	0	0
<b>18</b>	Load	1.001	-11.4	0	0	152	25
<b>19</b>	Load	1.034	-0.806	0	0	0	0
<b>20</b>	Load	0.972	-0.767	0	0	502	77
<b>21</b>	Load	1.009	-4.71	0	0	219	86
<b>22</b>	Load	1.028	0.06	0	0	0	0
<b>23</b>	Load	1.023	-0.091	0	0	216.5	63.6
<b>24</b>	Load	1.009	-7.472	0	0	285.6	-69.2



<b>25</b>	Load	1.014	-8.908	0	0	201	40.2	
<b>26</b>	Load	1.011	-16.08	0	0	139	17	
<b>27</b>	Load	1.001	-14.58	0	0	225	69.5	
<b>28</b>	Load	1.013	-22.32	0	0	183	20.6	
<b>29</b>	Load	1.013	-22.74	0	0	235.5	26.9	
<b>30</b>	constant voltage	1.018	-6.088	290	132.574	0	0	
<b>31</b>	swing	0.982	0	560.528	289.73	9.2	4.6	
<b>32</b>	constant voltage	0.943	2.297	650	144.86	0	0	
<b>33</b>	constant voltage	0.997	4.657	656.71	216.798	0	0	
<b>34</b>	constant voltage	0.982	4.722	508	103.11	0	0	
<b>35</b>	constant voltage	1.029	5.269	655.22	221.579	0	0	
<b>36</b>	constant voltage	1.044	8.195	567.566	109.405	0	0	
<b>37</b>	constant voltage	0.988	-0.997	580	20.298	0	0	
<b>38</b>	constant voltage	0.988	-22.74	0	0	0	0	
<b>39</b>	constant voltage	1	-8.119	1000	69.299	883	250	
				Total	5468.022	1307.653	5421.1	1303.9
				Percentage shed			11%	7%

**APPENDIX C:** Cost function figures for the optimal load shedding scheme.

Loss 163 MW from generator 2.

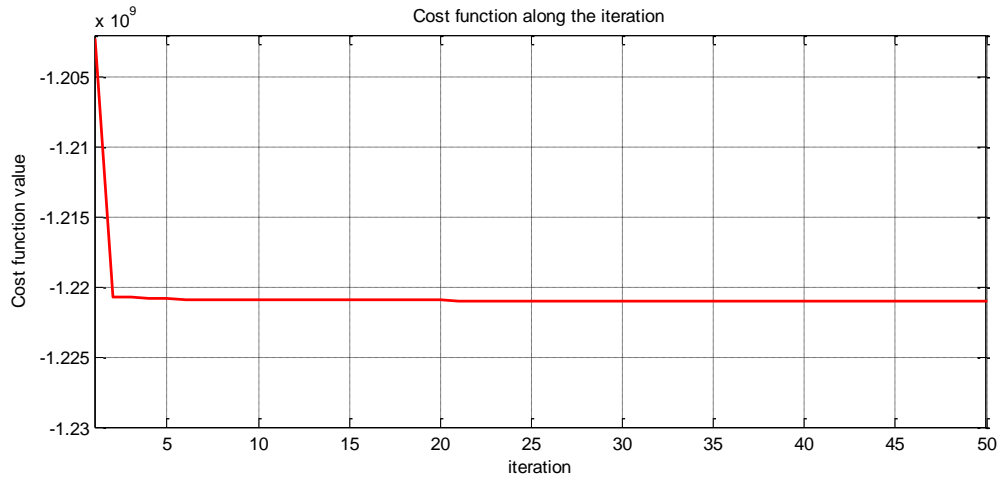


**Figure C.1 Loss 163 MW From generator 2.**

Loss 100 MW cost function

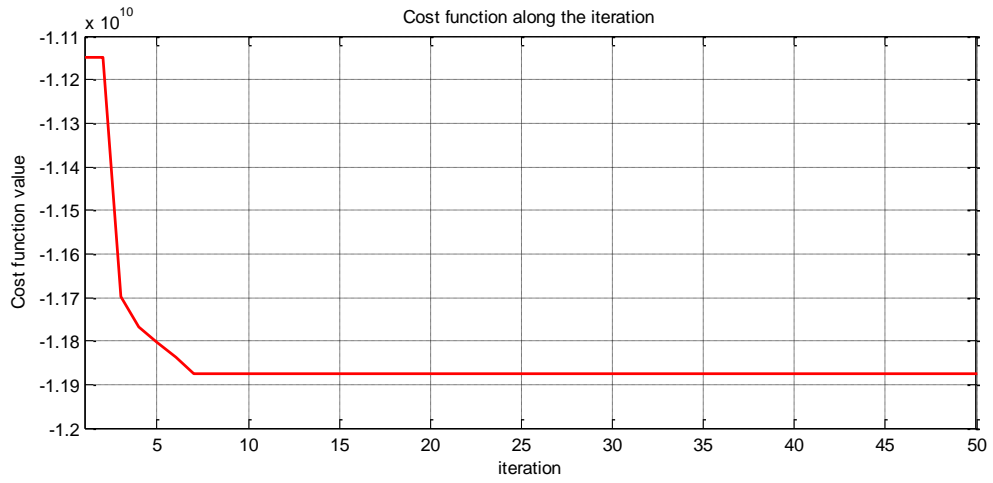


**Figure 0.2 Loss 100 MW cost function**

Loss 163 MW in presence of wind

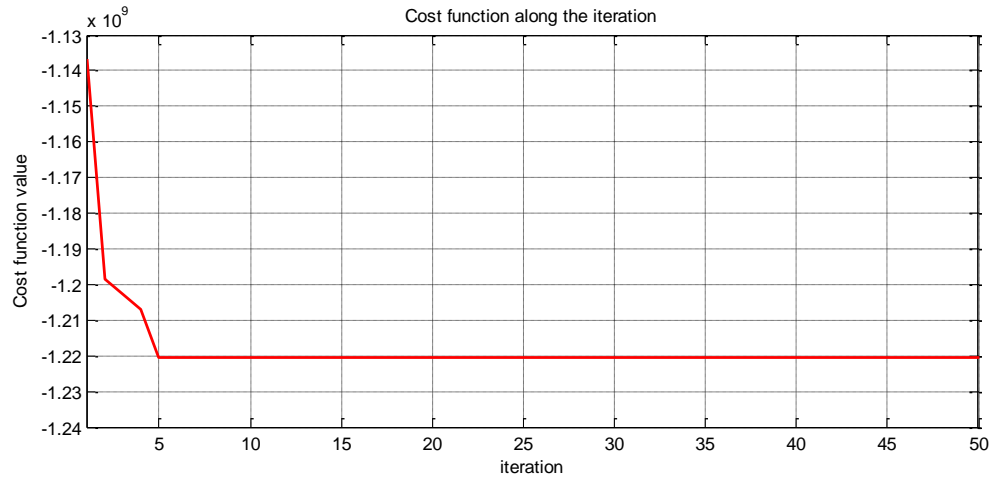


**Figure C.3 Loss 163 MW in presence of wind**

Loss transmission line 4-5

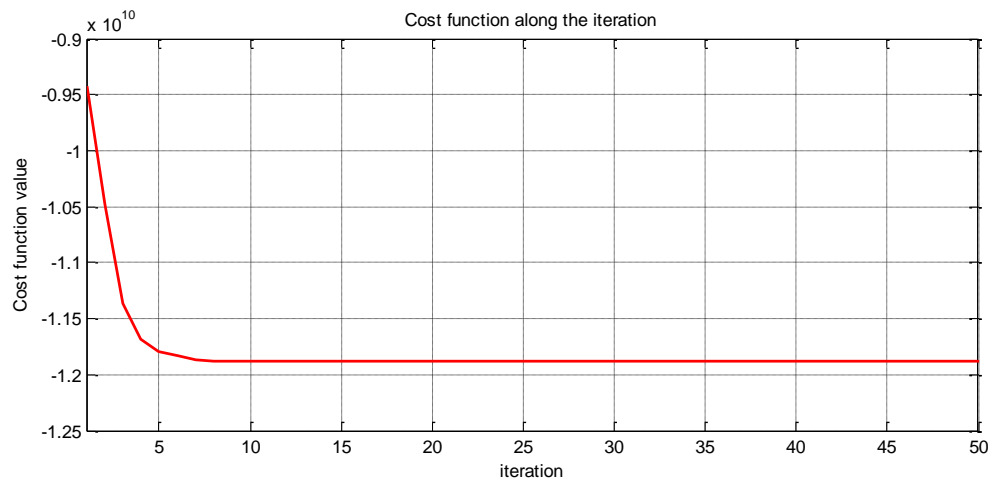


**Figure 0.4 Loss transmission line 4-5**

Loss generator 9 in 39 bus system

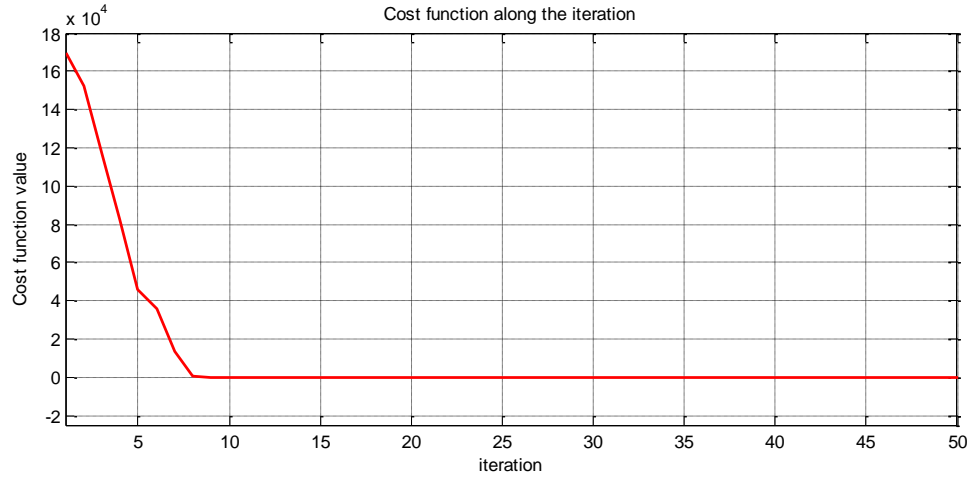


**Figure 0.5 Loss generator 9 in 39 bus system**

Loss generator 9 in 39 bus system in presence of wind

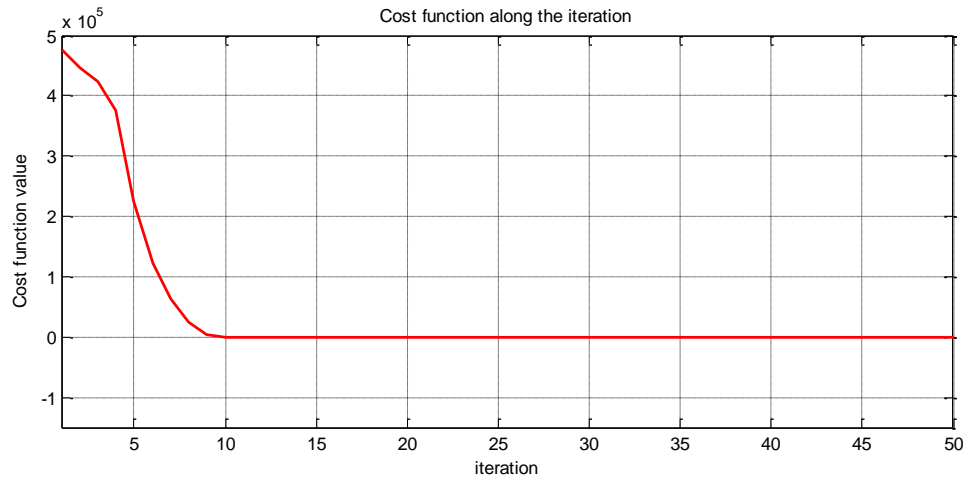


**Figure C.6 Loss generator 9 in 39 bus system in presence of wind**

Loss transmission lines 5-8 and 7-8

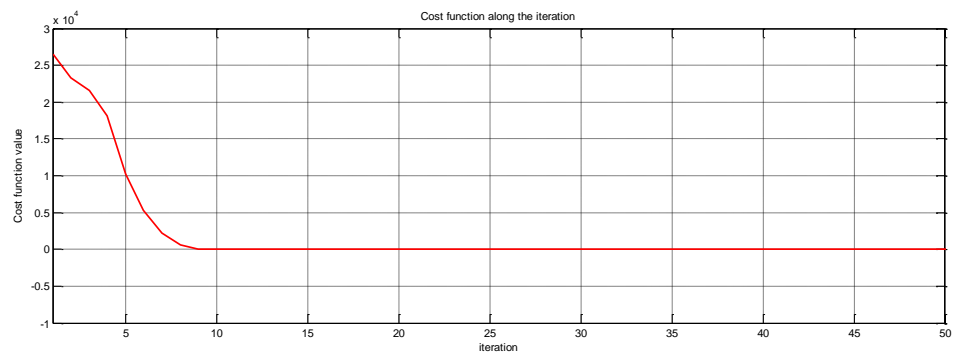


**Figure 0.7 Loss transmission lines 5-8 and 7-8**

## **Vitae**

Name : Shakir Dawalbait Ahmed Mohammed

Nationality : Sudanese

Date of Birth : 9/20/1987

Email : shikok0@hotmail.com

Address : King Fahd University of petroleum and Minerals,  
Dhahran, Saudi Arabia

Academic Background : BSc in Electrical Engineering from Sudan University of  
Science and Technology.